50th AIAA/ASME/ASCE/AHS/ASC Structures, Structural Dynamics, and Materials Conference
17th
4 - 7 May 2009, Palm Springs, California

AIAA 2009-2274

Recent Advances in Non-Intrusive Polynomial Chaos and Stochastic Collocation Methods for Uncertainty Analysis and Design

M. S. Eldred*
Sandia National Laboratories†, Albuquerque, NM 87185

Non-intrusive polynomial chaos expansion (PCE) and stochastic collocation (SC) methods are attractive techniques for uncertainty quantification (UQ) due to their strong mathematical basis and ability to produce functional representations of stochastic variability. PCE estimates coefficients for known orthogonal polynomial basis functions based on a set of response function evaluations, using sampling, linear regression, tensor-product quadrature, or Smolyak sparse grid approaches. SC, on the other hand, forms interpolation functions for known coefficients, and requires the use of structured collocation point sets derived from tensor product or sparse grids. When tailoring the basis functions or interpolation grids to match the forms of the input uncertainties, exponential convergence rates can be achieved with both techniques for a range of probabilistic analysis problems. In addition, analytic features of the expansions can be exploited for moment estimation and stochastic sensitivity analysis. In this paper, the latest ideas for tailoring these expansion methods to numerical integration approaches will be explored, in which expansion formulations are modified to best synchronize with tensor-product quadrature and Smolyak sparse grids using linear and nonlinear growth rules. The most promising stochastic expansion approaches are then carried forward for use in new approaches for mixed aleatory-epistemic UQ, employing second-order probability approaches, and design under uncertainty, employing bilevel, sequential, and multifidelity approaches.

I. Introduction

Uncertainty quantification (UQ) is the process of determining the effect of input uncertainties on response metrics of interest. These input uncertainties may be characterized as either aleatory uncertainties, which are irreducible variabilities inherent in nature, or epistemic uncertainties, which are reducible uncertainties resulting from a lack of knowledge. Since sufficient data is generally available for aleatory uncertainties, probabilistic methods are commonly used for computing response distribution statistics based on input probability distribution specifications. Conversely, for epistemic uncertainties, data is generally sparse, making the use of probability distribution assertions questionable and typically leading to nonprobabilistic methods based on interval specifications.

One technique for the analysis of aleatory uncertainties using probabilistic methods is the polynomial chaos expansion (PCE) approach to UQ. In this work, we focus on generalized polynomial chaos using the Wiener-Askey scheme,[1] in which Hermite, Legendre, Laguerre, Jacobi, and generalized Laguerre orthogonal polynomials are used for modeling the effect of uncertain variables described by normal, uniform, exponential, beta, and gamma probability distributions, respectively[a]. These orthogonal polynomial selections are optimal for these distribution types since the inner product weighting function and its corresponding support range correspond to the probability density functions for these continuous distributions. In theory, exponential convergence rates can be obtained with the optimal basis. When transformations to independent standard

*Principal Member of Technical Staff, Optimization and Uncertainty Estimation Department, MS-1318, Associate Fellow AIAA.

†Sandia is a multiprogram laboratory operated by Sandia Corporation, a Lockheed Martin Company, for the United States Department of Energy's National Nuclear Security Administration under Contract DE-AC04-94AL85000.

[a]Orthogonal polynomial selections also exist for discrete probability distributions, but are not explored here.

random variables (in some cases, approximated by uncorrelated standard random variables) are used, the variable expansions are uncoupled, allowing the polynomial orthogonality properties to be applied on a per-dimension basis. This allows one to mix and match the polynomial basis used for each variable without interference with the spectral projection scheme for the response.

In non-intrusive PCE, simulations are used as black boxes and the calculation of chaos expansion coefficients for response metrics of interest is based on a set of simulation response evaluations. To calculate these response PCE coefficients, two primary classes of approaches have been proposed: spectral projection and linear regression. The spectral projection approach projects the response against each basis function using inner products and employs the polynomial orthogonality properties to extract each coefficient. Each inner product involves a multidimensional integral over the support range of the weighting function, which can be evaluated numerically using sampling, quadrature, or sparse grid approaches. The linear regression approach (also known as point collocation or stochastic response surfaces) uses a single linear least squares solution to solve for the PCE coefficients which best match a set of response values obtained from a design of computer experiments.

Stochastic collocation (SC) is another stochastic expansion technique for UQ that is closely related to PCE. Whereas PCE estimates coefficients for known orthogonal polynomial basis functions, SC forms Lagrange interpolation functions for known coefficients. Since the i^{th} interpolation function is 1 at collocation point i and 0 for all other collocation points, it is easy to see that the expansion coefficients are just the response values at each of the collocation points. The formation of multidimensional interpolants with this property requires the use of structured collocation point sets derived from tensor products or sparse grids. The key to the approach is performing collocation using the Gauss points and weights from the same optimal orthogonal polynomials used in generalized PCE, which results in the same exponential convergence rates. A key distinction is that, whereas PCE must define an expansion formulation and a corresponding coefficient estimation approach (which may not be perfectly synchronized), SC requires only a collocation grid definition from which the expansion polynomials are derived based on Lagrange interpolation.

Once PCE or SC representations have been obtained for a response metric of interest, analytic expressions can be derived for the moments of the expansion (from integration over the aleatory random variables) and for the derivatives of these moments with respect to other variables, allowing for efficient design under uncertainty and mixed aleatory-epistemic UQ formulations involving moment control (e.g., robust design) or moment bounding (i.e., second-order interval estimation). To support tail statistics within reliability-based design or probability interval estimation, one simple approach employs projection of these analytic moments to compute approximate reliability indices (used herein), and more sophisticated approaches could involve analytic response PDF fitting based on Pearson/Johnson models using the first four moments (possible future work). This paper presents two approaches for calculation of sensitivities of moments with respect to nonprobabilistic dimensions (design or epistemic), one involving response function expansions over both probabilistic and nonprobabilistic variables and one involving response derivative expansions over only the probabilistic variables. In the former case, the dimensionality of the expansions is increased (requiring increased simulation runs to construct them), but the technique remains zeroth-order and the expansion spans the design/epistemic space (or potentially some subset of it). In the latter case, the expansion dimensionality is not increased, but accurate gradients with respect to the nonprobabilistic variables are now required for each simulation and the expansion over aleatory variables must be regenerated for each new design/epistemic point. The ability to compute analytic statistics and their derivatives using these two approaches enables bi-level, sequential, and multifidelity formulations to design under uncertainty and second-order probability approaches to mixed aleatory-epistemic UQ.

Section II describes the orthogonal polynomial and interpolation polynomial basis functions, Section III describes the generalized polynomial chaos and stochastic collocation methods, Section IV describes non-intrusive approaches for calculating the polynomial chaos coefficients or forming the set of stochastic collocation points, Section V presents approaches for higher level analyses based on stochastic expansions, Section VI describes a set of computational experiments, and Section VII provides concluding remarks.

II. Polynomial Basis

A. Orthogonal polynomials in the Askey scheme

Table 1 shows the set of polynomials which provide an optimal basis for different continuous probability distribution types. It is derived from the family of hypergeometric orthogonal polynomials known as the

Askey scheme,[2] for which the Hermite polynomials originally employed by Wiener[3] are a subset. The optimality of these basis selections derives from their orthogonality with respect to weighting functions that correspond to the probability density functions (PDFs) of the continuous distributions when placed in a standard form. The density and weighting functions differ by a constant factor due to the requirement that the integral of the PDF over the support range is one.

Table 1. Linkage between standard forms of continuous probability distributions and Askey scheme of continuous hyper-geometric polynomials.

Distribution	Density function	Polynomial	Weight function	Support range
Normal	$\frac{1}{\sqrt{2\pi}} e^{\frac{-x^2}{2}}$	Hermite $He_n(x)$	$e^{\frac{-x^2}{2}}$	$[-\infty, \infty]$
Uniform	$\frac{1}{2}$	Legendre $P_n(x)$	1	$[-1, 1]$
Beta	$\frac{(1-x)^\alpha (1+x)^\beta}{2^{\alpha+\beta+1} B(\alpha+1, \beta+1)}$	Jacobi $P_n^{(\alpha,\beta)}(x)$	$(1-x)^\alpha (1+x)^\beta$	$[-1, 1]$
Exponential	e^{-x}	Laguerre $L_n(x)$	e^{-x}	$[0, \infty]$
Gamma	$\frac{x^\alpha e^{-x}}{\Gamma(\alpha+1)}$	Generalized Laguerre $L_n^{(\alpha)}(x)$	$x^\alpha e^{-x}$	$[0, \infty]$

Note that Legendre is a special case of Jacobi for $\alpha = \beta = 0$, Laguerre is a special case of generalized Laguerre for $\alpha = 0$, $\Gamma(a)$ is the Gamma function which extends the factorial function to continuous values, and $B(a, b)$ is the Beta function defined as $B(a, b) = \frac{\Gamma(a)\Gamma(b)}{\Gamma(a+b)}$. Some care is necessary when specifying the α and β parameters for the Jacobi and generalized Laguerre polynomials since the orthogonal polynomial conventions[4] differ from the common statistical PDF conventions. The former conventions are used in Table 1.

B. Numerically generated orthogonal polynomials

If all random inputs can be described using independent normal, uniform, exponential, beta, and gamma distributions, then generalized PCE can be directly applied. If correlation or other distribution types are present, then additional techniques are required. One solution is to employ nonlinear variable transformations as described in Section III.C such that an Askey basis can be applied in the transformed space. This can be effective as shown in Ref. 5, but convergence rates are typically degraded. In addition, correlation coefficients are warped by the nonlinear transformation,[6] and transformed correlation values are not always readily available. An alternative is to numerically generate the orthogonal polynomials, along with their Gauss points and weights, that are optimal for given random variable sets having arbitrary probability density functions.[7,8] This not only preserves exponential convergence rates, it also eliminates the need to calculate correlation warping.

C. Interpolation polynomials

Lagrange polynomials interpolate a set of points in a single dimension using the functional form

$$L_j = \prod_{\substack{k=1 \\ k \neq j}}^{m} \frac{\xi - \xi_k}{\xi_j - \xi_k} \tag{1}$$

where it is evident that L_j is 1 at $\xi = \xi_j$, is 0 for each of the points $\xi = \xi_k$, and has order $m - 1$.

For interpolation of a response function R in one dimension over m points, the expression

$$R(\xi) \cong \sum_{j=1}^{m} r(\xi_j)\, L_j(\xi) \tag{2}$$

reproduces the response values $r(\xi_j)$ at the interpolation points and smoothly interpolates between these values at other points. For interpolation in multiple dimensions, a tensor-product approach is used wherein

$$R(\boldsymbol{\xi}) \cong \sum_{j_1=1}^{m_{i_1}} \cdots \sum_{j_n=1}^{m_{i_n}} r\left(\xi_{j_1}^{i_1}, \ldots, \xi_{j_n}^{i_n}\right) \left(L_{j_1}^{i_1} \otimes \cdots \otimes L_{j_n}^{i_n}\right) = \sum_{j=1}^{N_p} r_j(\boldsymbol{\xi}) \boldsymbol{L}_j(\boldsymbol{\xi}) \tag{3}$$

where $\boldsymbol{i} = (m_1, m_2, \cdots, m_n)$ are the number of nodes used in the n-dimensional interpolation and $\xi_{j_l}^{i_k}$ is the j_l-th point in the k-th direction. As will be seen later (Section IV.A.3), interpolation on sparse grids involves a summation of these tensor products with varying $\boldsymbol{i}$ levels.

III. Stochastic Expansion Methods

A. Generalized Polynomial Chaos

The set of polynomials from Section II.A are used as an orthogonal basis to approximate the functional form between the stochastic response output and each of its random inputs. The chaos expansion for a response R takes the form

$$R = a_0 B_0 + \sum_{i_1=1}^{\infty} a_{i_1} B_1(\xi_{i_1}) + \sum_{i_1=1}^{\infty} \sum_{i_2=1}^{i_1} a_{i_1 i_2} B_2(\xi_{i_1}, \xi_{i_2}) + \sum_{i_1=1}^{\infty} \sum_{i_2=1}^{i_1} \sum_{i_3=1}^{i_2} a_{i_1 i_2 i_3} B_3(\xi_{i_1}, \xi_{i_2}, \xi_{i_3}) + ... \tag{4}$$

where the random vector dimension is unbounded and each additional set of nested summations indicates an additional order of polynomials in the expansion. This expression can be simplified by replacing the order-based indexing with a term-based indexing

$$R = \sum_{j=0}^{\infty} \alpha_j \Psi_j(\boldsymbol{\xi}) \tag{5}$$

where there is a one-to-one correspondence between $a_{i_1 i_2 \ldots i_n}$ and α_j and between $B_n(\xi_{i_1}, \xi_{i_2}, ..., \xi_{i_n})$ and $\Psi_j(\boldsymbol{\xi})$. Each of the $\Psi_j(\boldsymbol{\xi})$ are multivariate polynomials which involve products of the one-dimensional polynomials. For example, a multivariate Hermite polynomial $B(\boldsymbol{\xi})$ of order n is defined from

$$B_n(\xi_{i_1}, ..., \xi_{i_n}) = e^{\frac{1}{2}\boldsymbol{\xi}^T \boldsymbol{\xi}} (-1)^n \frac{\partial^n}{\partial \xi_{i_1} \ldots \partial \xi_{i_n}} e^{-\frac{1}{2}\boldsymbol{\xi}^T \boldsymbol{\xi}} \tag{6}$$

which can be shown to be a product of one-dimensional Hermite polynomials involving a multi-index m_i^j:

$$B_n(\xi_{i_1}, ..., \xi_{i_n}) = \Psi_j(\boldsymbol{\xi}) = \prod_{i=1}^{n} \psi_{m_i^j}(\xi_i) \tag{7}$$

1. *Expansion truncation and tailoring*

In practice, one truncates the infinite expansion at a finite number of random variables and a finite expansion order

$$R \cong \sum_{j=0}^{P} \alpha_j \Psi_j(\boldsymbol{\xi}) \tag{8}$$

Traditionally, the polynomial chaos expansion includes a complete basis of polynomials up to a fixed total-order specification. For example, the multidimensional basis polynomials for a second-order expansion over two random dimensions are

$$\begin{aligned}
\Psi_0(\boldsymbol{\xi}) &= \psi_0(\xi_1)\, \psi_0(\xi_2) &&= 1 \\
\Psi_1(\boldsymbol{\xi}) &= \psi_1(\xi_1)\, \psi_0(\xi_2) &&= \xi_1 \\
\Psi_2(\boldsymbol{\xi}) &= \psi_0(\xi_1)\, \psi_1(\xi_2) &&= \xi_2 \\
\Psi_3(\boldsymbol{\xi}) &= \psi_2(\xi_1)\, \psi_0(\xi_2) &&= \xi_1^2 - 1 \\
\Psi_4(\boldsymbol{\xi}) &= \psi_1(\xi_1)\, \psi_1(\xi_2) &&= \xi_1 \xi_2 \\
\Psi_5(\boldsymbol{\xi}) &= \psi_0(\xi_1)\, \psi_2(\xi_2) &&= \xi_2^2 - 1
\end{aligned}$$

The total number of terms N_t in an expansion of total order p involving n random variables is given by

$$N_t = 1 + P = 1 + \sum_{s=1}^{p} \frac{1}{s!} \prod_{r=0}^{s-1} (n + r) = \frac{(n+p)!}{n!p!} \tag{9}$$

This traditional approach will be referred to as a "total-order expansion."

An important alternative approach is to employ a "tensor-product expansion," in which polynomial order bounds are applied on a per-dimension basis (no total-order bound is enforced) and all combinations of the one-dimensional polynomials are included. In this case, the example basis for $p = 2, n = 2$ is

$$\begin{aligned}
\Psi_0(\boldsymbol{\xi}) &= \psi_0(\xi_1)\,\psi_0(\xi_2) &&= 1 \\
\Psi_1(\boldsymbol{\xi}) &= \psi_1(\xi_1)\,\psi_0(\xi_2) &&= \xi_1 \\
\Psi_2(\boldsymbol{\xi}) &= \psi_2(\xi_1)\,\psi_0(\xi_2) &&= \xi_1^2 - 1 \\
\Psi_3(\boldsymbol{\xi}) &= \psi_0(\xi_1)\,\psi_1(\xi_2) &&= \xi_2 \\
\Psi_4(\boldsymbol{\xi}) &= \psi_1(\xi_1)\,\psi_1(\xi_2) &&= \xi_1\xi_2 \\
\Psi_5(\boldsymbol{\xi}) &= \psi_2(\xi_1)\,\psi_1(\xi_2) &&= (\xi_1^2 - 1)\xi_2 \\
\Psi_6(\boldsymbol{\xi}) &= \psi_0(\xi_1)\,\psi_2(\xi_2) &&= \xi_2^2 - 1 \\
\Psi_7(\boldsymbol{\xi}) &= \psi_1(\xi_1)\,\psi_2(\xi_2) &&= \xi_1(\xi_2^2 - 1) \\
\Psi_8(\boldsymbol{\xi}) &= \psi_2(\xi_1)\,\psi_2(\xi_2) &&= (\xi_1^2 - 1)(\xi_2^2 - 1)
\end{aligned}$$

and the total number of terms N_t is

$$N_t \;=\; 1 + P \;=\; \prod_{i=1}^{n} (p_i + 1) \tag{10}$$

where p_i is the polynomial order bound for the i-th dimension.

It is apparent from Eq. 10 that the tensor-product expansion readily supports anisotropy in polynomial order for each dimension, since the polynomial order bounds for each dimension can be specified independently. It is also feasible to support anisotropy with total-order expansions, although this involves pruning polynomials that satisfy the total-order bound (potentially defined from the maximum of the per-dimension bounds) but which violate individual per-dimension bounds. In this case, Eq. 9 does not apply.

Additional expansion form alternatives can also be considered. Of particular interest is the tailoring of expansion form to target specific monomial coverage as motivated by the integration process employed for evaluating chaos coefficients. If the specific monomial set that can be resolved by a particular integration approach is known or can be approximated, then the chaos expansion can be tailored to synchonize with this set. Tensor-product and total-order expansions can be seen as special cases of this general approach (corresponding to tensor-product quadrature and Smolyak sparse grids with linear growth rules, respectively), whereas, for example, Smolyak sparse grids with nonlinear growth rules could generate synchonized expansion forms that are neither tensor-product nor total-order (to be discussed later in association with Figure 3). In all cases, the specifics of the expansion are codified in the multi-index, and subsequent machinery for estimating response values at particular $\boldsymbol{\xi}$, evaluating response statistics by integrating over $\boldsymbol{\xi}$, etc., can be performed in a manner that is agnostic to the exact expansion formulation.

2. Dimension independence

A generalized polynomial basis is generated by selecting the univariate basis that is most optimal for each random input and then applying the products as defined by the multi-index to define a mixed set of multivariate polynomials. Similarly, multivariate weighting functions involve a product of the one-dimensional weighting functions and multivariate quadrature rules involve tensor products of the one-dimensional quadrature rules.

The use of independent standard random variables is the critical component that allows decoupling of the multidimensional integrals in a mixed basis expansion. It is assumed in this work that the uncorrelated standard random variables resulting from the transformation described in Section III.C can be treated as independent. This assumption is valid for uncorrelated standard normal variables (and motivates the approach of using a strictly Hermite basis), but may be an approximation for uncorrelated standard uniform, exponential, beta, and gamma variables. For independent variables, the multidimensional integrals involved in the inner products of multivariate polynomials decouple to a product of one-dimensional integrals involving only the particular polynomial basis and corresponding weight function selected for each random dimension. The multidimensional inner products are nonzero only if each of the one-dimensional inner products is nonzero, which preserves the desired multivariate orthogonality properties for the case of a mixed basis.

B. Stochastic Collocation

The SC expansion is formed as a sum of a set of multidimensional Lagrange interpolation polynomials, one polynomial per collocation point. Since these polynomials have the feature of being equal to 1 at their particular collocation point and 0 at all other points, the coefficients of the expansion are just the response values at each of the collocation points. This can be written as:

$$R \cong \sum_{j=1}^{N_p} r_j \boldsymbol{L}_j(\boldsymbol{\xi}) \tag{11}$$

where the set of N_p collocation points involves a structured multidimensional grid. There is no need for tailoring of the expansion form as there is for PCE (see Section III.A.1) since the polynomials that appear in the expansion are determined by the Lagrange construction (Eq. 1). That is, any tailoring or refinement of the expansion occurs through the selection of points in the interpolation grid and the polynomial orders of the basis adapt automatically.

As mentioned in Section I, the key to maximizing performance with this approach is to use the same Gauss points defined from the optimal orthogonal polynomials as the collocation points (using either a tensor product grid as shown in Eq. 3 or a sum of tensor products defined for a sparse grid as shown later in Section IV.A.3). Given the observation that Gauss points of an orthogonal polynomial are its roots, one can factor a one-dimensional orthogonal polynomial of order p as follows:

$$\psi_j = c_j \prod_{k=1}^{p} (\xi - \xi_k) \tag{12}$$

where ξ_k represent the roots. This factorization is very similar to Lagrange interpolation using Gauss points as shown in Eq. 1. However, to obtain a Lagrange interpolant of order p from Eq. 1 for each of the collocation points, one must use the roots of a polynomial that is one order higher (order $p+1$) and then exclude the Gauss point being interpolated. As discussed later in Section IV.A.2, one also uses these higher order $p+1$ roots to evaluate the PCE coefficient integrals for expansions of order p. Thus, the collocation points used for integration or interpolation for expansions of order p are the same; however, the polynomial bases for PCE (scaled polynomial product involving all p roots of order p) and SC (scaled polynomial product involving p root subset of order $p+1$) are closely related but not identical.

C. Transformations to uncorrelated standard variables

Polynomial chaos and stochastic collocation are expanded using polynomials that are functions of independent standard random variables $\boldsymbol{\xi}$. Thus, a key component of either approach is performing a transformation of variables from the original random variables $\boldsymbol{x}$ to independent standard random variables $\boldsymbol{\xi}$ and then applying the stochastic expansion in the transformed space. The dimension of $\boldsymbol{\xi}$ is typically chosen to correspond to the dimension of $\boldsymbol{x}$, although this is not required. In fact, the dimension of $\boldsymbol{\xi}$ should be chosen to represent the number of distinct sources of randomness in a particular problem, and if individual x_i mask multiple random inputs, then the dimension of $\boldsymbol{\xi}$ can be expanded to accommodate.[9] For simplicity, all subsequent discussion will assume a one-to-one correspondence between $\boldsymbol{\xi}$ and $\boldsymbol{x}$.

This notion of independent standard space is extended over the notion of "u-space" used in reliability methods[10,11] in that in includes not just independent standard normals, but also independent standardized uniforms, exponentials, betas and gammas. For problems directly involving independent normal, uniform, exponential, beta, and gamma distributions for input random variables, conversion to standard form involves a simple linear scaling transformation (to the form of the density functions in Table 1) and then the corresponding chaos/collocation points can be employed. For correlated normal, uniform, exponential, beta, and gamma distributions, the same linear scaling transformation is applied followed by application of the inverse Cholesky factor of the correlation matrix (similar to Eq. 14 below, but the correlation matrix requires no modification for linear transformations). As described previously, the subsequent independence assumption is valid for uncorrelated standard normals but may introduce error for uncorrelated standard uniform, exponential, beta, and gamma variables. For other distributions with a close relationship to variables supported in the Askey scheme (i.e., lognormal, loguniform, and triangular distributions), a nonlinear transformation is employed to transform to the corresponding Askey distributions (i.e., normal, uniform, and uniform distributions, respectively) and the corresponding chaos polynomials/collocation points are employed. For other

less directly-related distributions (e.g., extreme value distributions), the nonlinear Nataf transformation is employed to transform to uncorrelated standard normals as described below and Hermite polynomials are employed.

The transformation from correlated non-normal distributions to uncorrelated standard normal distributions is denoted as $\boldsymbol{\xi} = T(\mathbf{x})$ with the reverse transformation denoted as $\mathbf{x} = T^{-1}(\boldsymbol{\xi})$. These transformations are nonlinear in general, and possible approaches include the Rosenblatt,[12] Nataf,[6] and Box-Cox[13] transformations. The nonlinear transformations may also be linearized, and common approaches for this include the Rackwitz-Fiessler[14] two-parameter equivalent normal and the Chen-Lind[15] and Wu-Wirsching[16] three-parameter equivalent normals. The results in this paper employ the Nataf nonlinear transformation, which is suitable for the common case when marginal distributions and a correlation matrix are provided, but full joint distributions are not known[b]. The Nataf transformation occurs in the following two steps. To transform between the original correlated x-space variables and correlated standard normals ("z-space"), a CDF matching condition is applied for each of the marginal distributions:

$$\Phi(z_i) = F(x_i) \tag{13}$$

where $\Phi()$ is the standard normal cumulative distribution function and $F()$ is the cumulative distribution function of the original probability distribution. Then, to transform between correlated z-space variables and uncorrelated ξ-space variables, the Cholesky factor $\mathbf{L}$ of a modified correlation matrix is used:

$$\mathbf{z} = \mathbf{L}\boldsymbol{\xi} \tag{14}$$

where the original correlation matrix for non-normals in x-space has been modified to represent the corresponding "warped" correlation in z-space.[6]

IV. Non-intrusive methods for expansion formation

The major practical difference between PCE and SC is that, in PCE, one must estimate the coefficients for known basis functions, whereas in SC, one must form the interpolants for known coefficients. PCE estimates its coefficients using any of the approaches to follow: random sampling, tensor-product quadrature, Smolyak sparse grids, or linear regression. In SC, the multidimensional interpolants need to be formed over structured data sets, such as point sets from quadrature or sparse grids; approaches based on random sampling may not be used.

A. Spectral projection

The spectral projection approach projects the response against each basis function using inner products and employs the polynomial orthogonality properties to extract each coefficient. Similar to a Galerkin projection, the residual error from the approximation is rendered orthogonal to the selected basis. From Eq. 8, it is evident that

$$\alpha_j \;=\; \frac{\langle R, \Psi_j \rangle}{\langle \Psi_j^2 \rangle} \;=\; \frac{1}{\langle \Psi_j^2 \rangle} \int_\Omega R\, \Psi_j\, \varrho(\boldsymbol{\xi})\, d\boldsymbol{\xi}, \tag{15}$$

where each inner product involves a multidimensional integral over the support range of the weighting function. In particular, $\Omega = \Omega_1 \otimes \cdots \otimes \Omega_n$, with possibly unbounded intervals $\Omega_j \subset \mathbb{R}$ and the tensor product form $\varrho(\boldsymbol{\xi}) = \prod_{i=1}^n \varrho_i(\xi_i)$ of the joint probability density (weight) function. The denominator in Eq. 15 is the norm squared of the multivariate orthogonal polynomial, which can be computed analytically using the product of univariate norms squared

$$\langle \Psi_j^2 \rangle \;=\; \prod_{i=1}^{n} \langle \psi_{m_i^j}^2 \rangle \tag{16}$$

where the univariate inner products have simple closed form expressions for each polynomial in the Askey scheme.[4] Thus, the primary computational effort resides in evaluating the numerator, which is evaluated numerically using sampling, quadrature or sparse grid approaches (and this numerical approximation leads to use of the term "pseudo-spectral" by some investigators).

[b] If joint distributions are known, then the Rosenblatt transformation is preferred.

1. Sampling

In the sampling approach, the integral evaluation is equivalent to computing the expectation (mean) of the response-basis function product (the numerator in Eq. 15) for each term in the expansion when sampling within the density of the weighting function. This approach is only valid for PCE and since sampling does not provide any particular monomial coverage guarantee, it is common to combine this coefficient estimation approach with a total-order chaos expansion.

In computational practice, coefficient estimations based on sampling benefit from first estimating the response mean (the first PCE coefficient) and then removing the mean from the expectation evaluations for all subsequent coefficients.[9] While this has no effect for quadrature/sparse grid methods (see following two sections) and little effect for fully-resolved sampling, it does have a small but noticeable beneficial effect for under-resolved sampling.

2. Tensor product quadrature

In quadrature-based approaches, the simplest general technique for approximating multidimensional integrals, as in Eq. 15, is to employ a tensor product of one-dimensional quadrature rules. In the case where Ω is a hypercube, i.e. $\Omega = [-1, 1]^n$, there are several choices of nested abscissas, included Clenshaw-Curtis, Gauss-Patterson, etc.[17–19] However, in the tensor-product case, we choose Gaussian abscissas, i.e. the zeros of polynomials that are orthogonal with respect to a density function weighting, e.g. Gauss-Hermite, Gauss-Legendre, Gauss-Laguerre, generalized Gauss-Laguerre, and Gauss-Jacobi.

We first introduce an index $i \in \mathbb{N}_+$, $i \geq 1$. Then, for each value of i, let $\{\xi_1^i, \ldots, \xi_{m_i}^i\} \subset \Omega_i$ be a sequence of abscissas for quadrature on Ω_i. For $f \in C^0(\Omega_i)$ and $n = 1$ we introduce a sequence of one-dimensional quadrature operators

$$\mathscr{U}^i(f)(\xi) = \sum_{j=1}^{m_i} f(\xi_j^i)\, w_j^i, \tag{17}$$

with $m_i \in \mathbb{N}$ given. When utilizing Gaussian quadrature, Eq. 17 integrates exactly all polynomials of degree less than or equal to $2m_i - 1$, for each $i = 1, \ldots, n$. Given an expansion order p, the highest order coefficient evaluations (Eq. 15) can be assumed to involve integrands of at least polynomial order $2p$ (Ψ of order p and R modeled to order p) in each dimension such that a minimal Gaussian quadrature order of $p + 1$ will be required to obtain good accuracy in these coefficients.

Now, in the multivariate case $n > 1$, for each $f \in C^0(\Omega)$ and the multi-index $\mathbf{i} = (i_1, \ldots, i_n) \in \mathbb{N}_+^n$ we define the full tensor product quadrature formulas

$$\mathcal{Q}_{\mathbf{i}}^n f(\xi) = \left(\mathscr{U}^{i_1} \otimes \cdots \otimes \mathscr{U}^{i_n}\right)(f)(\boldsymbol{\xi}) = \sum_{j_1=1}^{m_{i_1}} \cdots \sum_{j_n=1}^{m_{i_n}} f\left(\xi_{j_1}^{i_1}, \ldots, \xi_{j_n}^{i_n}\right) \left(w_{j_1}^{i_1} \otimes \cdots \otimes w_{j_n}^{i_n}\right). \tag{18}$$

Clearly, the above product needs $\prod_{j=1}^n m_{i_j}$ function evaluations. Therefore, when the number of input random variables is small, full tensor-product quadrature is a very effective numerical tool. On the other hand, approximations based on tensor-product grids suffer from the *curse of dimensionality* since the number of collocation points in a tensor grid grows exponentially fast in the number of input random variables. For example, if Eq. 18 employs the same order for all random dimensions, $m_{i_j} = m$, then Eq. 18 requires m^n function evaluations.

Figure 1 displays the monomial coverage for an integrand evaluated using an isotropic Gaussian quadrature rules in two dimensions ($m_1 = m_2 = 5$). Given this type of coverage, the traditional approach of exploying a total-order chaos expansion (involving integrands indicated by the red horizontal line) neglects a significant portion of the monomial coverage and one would expect a tensor-product expansion to provide improved synchronization and more effective usage of the Gauss point evaluations. Note that the integrand monomial coverage must resolve $2p$, such that $p_1 = p_2 = 4$ would be selected in this case.

3. Smolyak sparse grids

If the number of random variables is moderately large, one should rather consider sparse tensor product spaces as first proposed by Smolyak[20] and further investigated by Refs. 17–19, 21–23 that reduce dramatically the number of collocation points, while preserving a high level of accuracy.

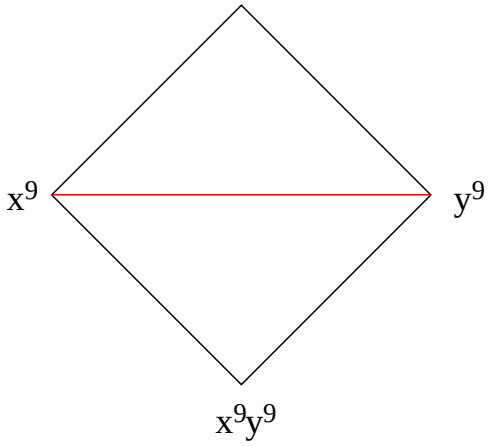

Figure 1. Pascal's triangle depiction of integrand monomial coverage for two dimensions and Gaussian tensor-product quadrature order = 5. Red line depicts maximal total-order integrand coverage.

Here we follow the notation and extend the description in Ref. 17 to describe the Smolyak *isotropic* formulas $\mathscr{A}(\mathrm{w}, n)$, where w is a level that is independent of dimension[c]. The Smolyak formulas are just linear combinations of the product formulas in Eq. 18 with the following key property: only products with a relatively small number of points are used. With $\mathscr{U}^0 = 0$ and for $i \geq 1$ define

$$\Delta^i = \mathscr{U}^i - \mathscr{U}^{i-1}. \tag{19}$$

and we set $|\mathbf{i}| = i_1 + \cdots + i_n$. Then the isotropic Smolyak quadrature formula is given by

$$\mathscr{A}(\mathrm{w}, n) = \sum_{|\mathbf{i}| \leq \mathrm{w}+n} \left(\Delta^{i_1} \otimes \cdots \otimes \Delta^{i_n} \right). \tag{20}$$

Equivalently, formula Eq. 20 can be written as[24]

$$\mathscr{A}(\mathrm{w}, n) = \sum_{\mathrm{w}+1 \leq |\mathbf{i}| \leq \mathrm{w}+n} (-1)^{\mathrm{w}+n-|\mathbf{i}|} \binom{n-1}{\mathrm{w}+n-|\mathbf{i}|} \cdot \left(\mathscr{U}^{i_1} \otimes \cdots \otimes \mathscr{U}^{i_n} \right). \tag{21}$$

Given an index set of levels, linear or nonlinear growth rules may be defined for the one-dimensional quadrature orders in order to take advantage of nesting of collocation points. The following growth rules are currently available for indices $i \geq 1$:

$$\text{Clenshaw} - \text{Curtis}: \quad m = \begin{cases} 1 & i = 1 \\ 2^{i-1} + 1 & i > 1 \end{cases} \tag{22}$$

$$\text{Gaussian nonlinear}: \quad m = 2^i - 1 \tag{23}$$

$$\text{Gaussian linear}: \quad m = 2i - 1 \tag{24}$$

For fully nested quadrature rules such as Clenshaw-Curtis and Gauss-Patterson, nonlinear growth rules are strongly preferred (Eq. 22 for the former and Eq. 23 for the latter). For at most weakly nested Gaussian quadrature rules, either linear or nonlinear rules may be selected, with the former motivated by finer granularity of control and uniform integrand coverage and the latter motivated by consistency with Clenshaw-Curtis and Gauss-Patterson. The $m = 2i - 1$ linear rule takes advantage of weak nesting (e.g., Gauss-Hermite and Gauss-Legendre), whereas non-nested rules (e.g., Gauss-Laguerre) could alternatively employ an $m = i$ linear rule without any loss of reuse. In the experiments to follow, Clenshaw-Curtis employs nonlinear growth via Eq. 22, and all Gaussian rules employ either nonlinear growth from Eq. 23 or linear growth from Eq. 24.

[c]Other common formulations use a dimension-dependent level q where $q \geq n$. We use $\mathrm{w} = q - n$, where $\mathrm{w} \geq 0$ for all n.

Examples of isotropic sparse grids, constructed from the fully nested Clenshaw-Curtis abscissas and the weakly-nested Gaussian abscissas are shown in Figure 2, where $\Omega = [-1, 1]^2$. There, we consider a two-dimensional parameter space and a maximum level w = 5 (sparse grid $\mathscr{A}(5, 2)$). To see the reduction in function evaluations with respect to full tensor product grids, we also include a plot of the corresponding Clenshaw-Curtis isotropic full tensor grid having the same maximum number of points in each direction, namely $2^5 + 1 = 33$. Whereas an isotropic tensor-product quadrature scales as m^n, an isotropic sparse grid scales as $m^{\log\, n}$, significantly mitigating the curse of dimensionality.

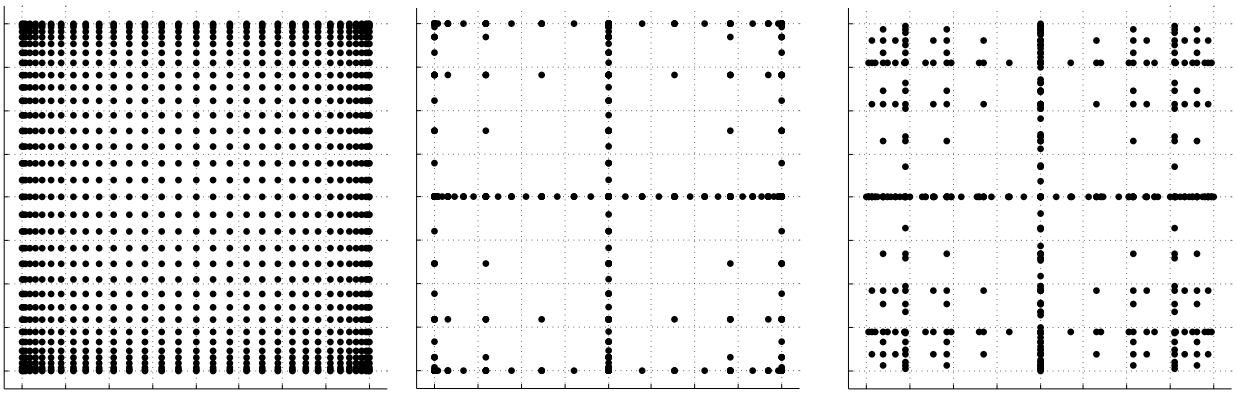

Figure 2. For a two-dimensional parameter space ($n = 2$) and maximum level w = 5, we plot the full tensor product grid using the Clenshaw-Curtis abscissas (left) and isotropic Smolyak sparse grids $\mathscr{A}(5, 2)$, utilizing the Clenshaw-Curtis abscissas (middle) and the Gaussian abscissas (right).

Figure 3 displays the monomial coverage in Pascal's triangle for an isotropic sparse grid with level $w = 4$ employing Gaussian integration rules in two dimensions. Given this geometric interpretation, subtracted tensor-product grids from Eqs. 20 and 21 can be interpreted as regions of overlap where only a single contribution to the integral should be retained. Figure 3(a) shows the case of nonlinear growth rules as given in Eq. 23 and Figure 3(b) shows the linear growth rule given in Eq. 24. Given this type of coverage, the traditional approach of exploying a total-order chaos expansion (maximal resolvable total-order integrand depicted with red horizontal line) can be seen to be well synchronized for the case of linear growth rules, since only a few small "teeth" protrude beyond the maximal total-order basis, and to be somewhat conservative for nonlinear growth rules, since the maximal total-order basis is dictated by the concave interior and neglects the outer "legs." However, the inclusion of additional terms beyond the total-order basis in the nonlinear growth rule case, as motivated by the legs in Figure 3(a), is error-prone, since the order of the unknown response function will tend to push the product integrand out into the concave interior, resulting in product polynomials that are not resolvable by the sparse integration. For the total-order basis, the integrand monomial coverage must resolve $2p$, such that $p = 9$ would be selected in the nonlinear growth rule case and $p = 7$ would be selected in the linear growth rule case.

B. Linear regression

The linear regression approach (also known as point collocation or stochastic response surfaces[25,26]) uses a single linear least squares solution of the form:

$$\boldsymbol{\Psi\alpha} = \boldsymbol{R} \tag{25}$$

to solve for the complete set of PCE coefficients $\boldsymbol{\alpha}$ that best match a set of response values $\boldsymbol{R}$. The set of response values is typically obtained by performing a design of computer experiments within the density function of $\boldsymbol{\xi}$, where each row of the matrix $\boldsymbol{\Psi}$ contains the N_t multivariate polynomial terms Ψ_j evaluated at a particular $\boldsymbol{\xi}$ sample. An over-sampling is generally advisable (Ref. 26 recommends $2N_t$ samples), resulting in a least squares solution for the over-determined system. In the case of $2N_t$ oversampling, the simulation requirements for this approach scale as $\frac{2(n+p)!}{n!p!}$, which can be significantly more affordable than isotropic tensor-product quadrature (e.g., $(p+1)^n$) for larger problems. As for sampling-based coefficient estimation,

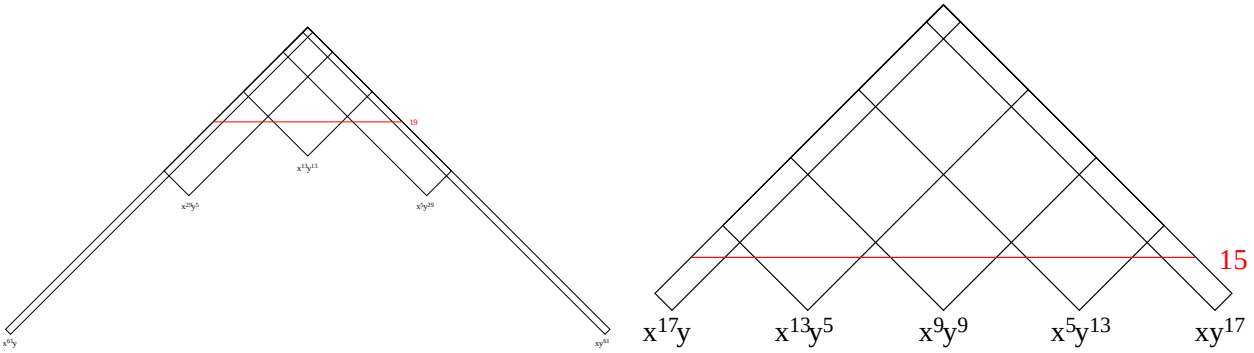

(a) Nonlinear growth rule.

(b) Linear growth rule.

Figure 3. Pascal's triangle depiction of integrand monomial coverage for two dimensions and Gaussian sparse grid level = 4. Red line depicts maximal total-order integrand coverage.

this approach is only valid for PCE and does not provide any particular monomial coverage guarantee; thus it is common to combine this coefficient estimation approach with a total-order chaos expansion.

A closely related technique is known as the "probabilistic collocation" approach. Rather than employing random over-sampling, this technique uses a selected subset of N_t Gaussian quadrature points (those with highest tensor-product weighting), which provides more optimal collocation locations and preserves interpolation properties.

Finally, additional regression equations can be obtained through the use of derivative information (gradients and Hessians) from each collocation point, which aids greatly in scaling with respect to the number of random variables.

V. Nonprobabilistic Extensions to Stochastic Expansions

A. Stochastic Sensitivity Analysis

Stochastic expansion methods have a number of convenient analytic features that make them attractive for use within higher level analyses, such as local and global sensitivity analysis, mixed aleatory/epistemic uncertainty quantification, and design under uncertainty algorithms. First, moments of the response expansion are available analytically. Second, the response expansions are readily differentiated with respect to the underlying expansion variables, and response moment expressions are readily differentiated with respect to auxilliary nonprobabilistic variables.

1. Analytic moments

Mean and variance of the polynomial chaos expansion are available in simple closed form:

$$\mu_R = \langle R \rangle \cong \sum_{j=0}^{P} \alpha_j \langle \Psi_j(\boldsymbol{\xi}) \rangle = \alpha_0 \tag{26}$$

$$\sigma_R^2 = \langle (R - \mu_R)^2 \rangle \cong \langle (\sum_{j=1}^{P} \alpha_j \Psi_j(\boldsymbol{\xi}))^2 \rangle = \sum_{j=1}^{P} \sum_{k=1}^{P} \alpha_j \alpha_k \langle \Psi_j(\boldsymbol{\xi}) \Psi_k(\boldsymbol{\xi}) \rangle = \sum_{j=1}^{P} \alpha_j^2 \langle \Psi_j^2 \rangle \tag{27}$$

where the norm squared of each multivariate polynomial is computed from Eq. 16. The moments μ_R and σ_R are exact moments of the expansion, which converge to moments of the true response function. Higher moments are also available analytically and could be employed in moment fitting approaches (i.e., Pearson and Johnson models) in order to approximate a response PDF, although this is outside the scope of the current paper.

Similar expressions can be derived for stochastic collocation:

$$\mu_R = \langle R \rangle \cong \sum_{j=1}^{N_p} r_j \langle \boldsymbol{L}_j(\boldsymbol{\xi}) \rangle = \sum_{j=1}^{N_p} r_j w_j \tag{28}$$

$$\sigma_R^2 = \langle R^2 \rangle - \mu_R^2 \cong \sum_{j=1}^{N_p} \sum_{k=1}^{N_p} r_j r_k \langle \boldsymbol{L}_j(\boldsymbol{\xi}) \boldsymbol{L}_k(\boldsymbol{\xi}) \rangle - \mu_R^2 = \sum_{j=1}^{N_p} r_j^2 w_j - \mu_R^2 \tag{29}$$

where the expectation of a particular Lagrange polynomial constructed at Gauss points and then integrated at these same Gauss points leaves only the weight corresponding to the point for which the interpolation value is one.

2. Global sensitivity analysis: interpretation of PCE coefficients

In the case of PCE, the chaos coefficients provide information on the global sensitivity of the response with respect to the expansion variables. As described in Ref. 27, variance-based decomposition has much in common with expansions based on orthogonal polynomial bases, and it is straighforward to analytically compute Sobol' sensitivity indices from the set of PCE coefficients as a post-processing step. This allows an assessment of which expansion variables are most influential in contributing to the output uncertainty.

3. Local sensitivity analysis: derivatives with respect to expansion variables

Polynomial chaos expansions are easily differentiated with respect to the random variables.[28] First, using Eq. 8,

$$\frac{dR}{d\xi_i} \cong \sum_{j=0}^{P} \alpha_j \frac{d\Psi_j(\boldsymbol{\xi})}{d\xi_i} \tag{30}$$

and then using Eq. 7,

$$\frac{d\Psi_j(\boldsymbol{\xi})}{d\xi_i} = \frac{d\psi_i}{d\xi_i} \prod_{\substack{k=1 \\ k \neq i}}^{n} \psi_{m_k^j}(\xi_k) \tag{31}$$

where the univariate polynomial derivatives $\frac{d\psi_i}{d\xi_i}$ have simple closed form expressions for each polynomial in the Askey scheme.[4] Finally, using the Jacobian of the Nataf variable transformation,

$$\frac{dR}{dx_i} = \frac{dR}{d\boldsymbol{\xi}} \frac{d\boldsymbol{\xi}}{dx_i} \tag{32}$$

which simplifies to $\frac{dR}{d\xi_i} \frac{d\xi_i}{dx_i}$ in the case of uncorrelated x_i.

Similar expressions may be derived for stochastic collocation, starting from Eq. 11:

$$\frac{dR}{d\xi_i} = \sum_{j=1}^{N_p} r_j \frac{d\boldsymbol{L}_j(\boldsymbol{\xi})}{d\xi_i} \tag{33}$$

where the multidimensional interpolant $\boldsymbol{L}_j$ is formed over either tensor-product quadrature points or a Smolyak sparse grid. For the former case, the derivative of the multidimensional interpolant $\boldsymbol{L}_j$ involves a product rule of the one-dimensional interpolants L_k:

$$\frac{d\boldsymbol{L}_j(\boldsymbol{\xi})}{d\xi_i} = \frac{dL_i}{d\xi_i} \prod_{\substack{k=1 \\ k \neq i}}^{n} L_k(\xi_k) \tag{34}$$

and for the latter case, the derivative involves a linear combination of these product rules, as dictated by the Smolyak recursion shown in Eq. 21. Finally, calculation of $\frac{dR}{dx_i}$ involves the same Jacobian application shown in Eq. 32.

4. Local sensitivity analysis: derivatives of probabilistic expansions with respect to nonprobabilistic variables

With the introduction of nonprobabilistic variables $\boldsymbol{s}$ (for example, design variables or epistemic uncertain variables), a polynomial chaos expansion only over the random variables $\boldsymbol{\xi}$ has the functional relationship:

$$R(\boldsymbol{\xi}, \boldsymbol{s}) \cong \sum_{j=0}^{P} \alpha_j(\boldsymbol{s}) \Psi_j(\boldsymbol{\xi}) \tag{35}$$

In this case, sensitivities of the mean and variance in Eqs. 26 and 27 with respect to the nonprobabilistic variables are as follows:

$$\frac{d\mu_R}{ds} = \frac{d\alpha_0}{ds} = \frac{d}{ds}\langle R \rangle = \langle \frac{dR}{ds} \rangle \tag{36}$$

$$\frac{d\sigma_R^2}{ds} = \sum_{j=1}^{P} \langle \Psi_j^2 \rangle \frac{d\alpha_j^2}{ds} = 2 \sum_{j=1}^{P} \alpha_j \langle \frac{dR}{ds}, \Psi_j \rangle \tag{37}$$

since

$$\frac{d\alpha_j}{ds} = \frac{\langle \frac{dR}{ds}, \Psi_j \rangle}{\langle \Psi_j^2 \rangle} \tag{38}$$

The coefficients calculated in Eq. 38 may be interpreted as either the nonprobabilistic sensitivities of the chaos coefficients for the response expansion or the chaos coefficients of an expansion for the nonprobabilistic sensitivities of the response. The evaluation of integrals involving $\frac{dR}{ds}$ extends the data requirements for the PCE approach to include response sensitivities at each of the sampling points for the quadrature, sparse grid, sampling, or point collocation coefficient estimation approaches. The resulting expansions are valid only for a particular set of nonprobabilistic variables and must be recalculated each time the nonprobabilistic variables are modified.

Similarly for stochastic collocation,

$$R(\boldsymbol{\xi}, \boldsymbol{s}) \cong \sum_{j=1}^{N_p} r_j(\boldsymbol{s}) \boldsymbol{L}_j(\boldsymbol{\xi}) \tag{39}$$

leads to

$$\frac{d\mu_R}{ds} = \frac{d}{ds}\langle R \rangle = \sum_{j=1}^{N_p} \frac{dr_j}{ds} \langle \boldsymbol{L}_j \rangle = \sum_{j=1}^{N_p} w_j \frac{dr_j}{ds} \tag{40}$$

$$\frac{d\sigma_R^2}{ds} = \sum_{j=1}^{N_p} 2 w_j r_j \frac{dr_j}{ds} - 2\mu_R \frac{d\mu_R}{ds} = \sum_{j=1}^{N_p} 2 w_j (r_j - \mu_R) \frac{dr_j}{ds} \tag{41}$$

based on differentiation of Eqs. 28-29.

5. Local sensitivity analysis: derivatives of combined expansions with respect to nonprobabilistic variables

Alternatively, a stochastic expansion can be formed over both $\boldsymbol{\xi}$ and $\boldsymbol{s}$. Assuming a bounded domain $\boldsymbol{s}_L \leq \boldsymbol{s} \leq \boldsymbol{s}_U$ (with no implied probability content) for the nonprobabilistic variables, a Legendre chaos basis would be appropriate for each of the dimensions in $\boldsymbol{s}$ within a polynomial chaos expansion.

$$R(\boldsymbol{\xi}, \boldsymbol{s}) \cong \sum_{j=0}^{P} \alpha_j \Psi_j(\boldsymbol{\xi}, \boldsymbol{s}) \tag{42}$$

In this case, sensitivities for the mean and variance do not require response sensitivity data, but this comes at the cost of forming the PCE over additional dimensions. For this combined variable expansion, the mean and variance are evaluated by performing the expectations over only the probabilistic expansion variables,

which eliminates the polynomial dependence on $\boldsymbol{\xi}$, leaving behind the desired polynomial dependence of the moments on $\boldsymbol{s}$:

$$\mu_R(\boldsymbol{s}) = \sum_{j=0}^{P} \alpha_j \langle \Psi_j(\boldsymbol{\xi}, \boldsymbol{s}) \rangle_{\boldsymbol{\xi}} \tag{43}$$

$$\sigma_R^2(\boldsymbol{s}) = \sum_{j=0}^{P} \sum_{k=0}^{P} \alpha_j \alpha_k \langle \Psi_j(\boldsymbol{\xi}, \boldsymbol{s}) \Psi_k(\boldsymbol{\xi}, \boldsymbol{s}) \rangle_{\boldsymbol{\xi}} \; - \; \mu_R^2(\boldsymbol{s}) \tag{44}$$

The remaining polynomials may then be differentiated with respect to $\boldsymbol{s}$. In this approach, the combined PCE is valid for the full nonprobabilistic variable range ($\boldsymbol{s}_L \leq \boldsymbol{s} \leq \boldsymbol{s}_U$) and does not need to be updated for each change in nonprobabilistic variables, although adaptive localization techniques (i.e., trust region model management approaches) can be employed when improved local accuracy of the sensitivities is required.

Similarly for stochastic collocation,

$$R(\boldsymbol{\xi}, \boldsymbol{s}) \cong \sum_{j=1}^{N_p} r_j \boldsymbol{L}_j(\boldsymbol{\xi}, \boldsymbol{s}) \tag{45}$$

leads to

$$\mu_R(\boldsymbol{s}) = \sum_{j=1}^{N_p} r_j \langle \boldsymbol{L}_j(\boldsymbol{\xi}, \boldsymbol{s}) \rangle_{\boldsymbol{\xi}} \tag{46}$$

$$\sigma_R^2(\boldsymbol{s}) = \sum_{j=1}^{N_p} \sum_{k=1}^{N_p} r_j r_k \langle \boldsymbol{L}_j(\boldsymbol{\xi}, \boldsymbol{s}) \boldsymbol{L}_k(\boldsymbol{\xi}, \boldsymbol{s}) \rangle_{\boldsymbol{\xi}} \; - \; \mu_R^2(\boldsymbol{s}) \tag{47}$$

where the remaining polynomials not eliminated by the expectation over $\boldsymbol{\xi}$ are again differentiated with respect to $\boldsymbol{s}$.

6. Inputs and outputs

There are two types of nonprobabilistic variables for which sensitivities must be calculated: "augmented," where the nonprobabilistic variables are separate from and augment the probabilistic variables, and "inserted," where the nonprobabilistic variables define distribution parameters for the probabilistic variables. While one could artificially augment the dimensionality of a combined variable expansion approach with inserted nonprobabilistic variables, this is not currently explored in this paper. Thus, any inserted nonprobabilistic variable sensitivities must be handled using Eqs. 36-37 and Eqs. 40-41 where $\frac{dR}{ds}$ is calculated as $\frac{dR}{dx}\frac{dx}{ds}$ and $\frac{dx}{ds}$ is the Jacobian of the variable transformation $\mathbf{x} = T^{-1}(\boldsymbol{\xi})$ with respect to the inserted nonprobabilistic variables.

While moment sensitivities directly enable robust design optimization formulations which seek to control response variance, design for reliability requires design sensitivities of tail statistics. In this abstract, we initially focus on design sensitivity of simple moment projections for this purpose. In reliability analysis using the Mean Value method, forward ($\bar{z} \rightarrow \beta$) and inverse ($\bar{\beta} \rightarrow z$) mappings employing the reliability index are approximated as:[10,11]

$$\beta_{cdf} = \frac{\mu_R - \bar{z}}{\sigma_R} \tag{48}$$

$$\beta_{ccdf} = \frac{\bar{z} - \mu_R}{\sigma_R} \tag{49}$$

$$z = \mu_R - \sigma_R \bar{\beta}_{cdf} \tag{50}$$

$$z = \mu_R + \sigma_R \bar{\beta}_{ccdf} \tag{51}$$

such that it is straightforward to form approximate design sensitivities of β and z from the PCE moment sensitivities. From here, approximate design sensitivities of probability levels may also be formed given a probability expression (such as $\Phi(-\beta)$) for the reliability index. The current alternative of numerical design

sensitivities of sampled probability levels would employ fewer simplifying approximations, but would also be much more expensive to compute accurately and is avoided for now. Future capabilities for analytic probability sensitivities could be based on Pearson/Johnson model for analytic response PDFs or sampling sensitivity approaches.

B. Optimization Formulations

Given the capability to compute analytic statistics of the response along with design sensitivities of these statistics, we pursue bi-level, sequential, and multifidelity approaches for optimization under uncertainty (OUU). The latter two approaches apply surrogate modeling approaches (data fits and multifidelity modeling) to the uncertainty analysis and then apply trust region model management to the optimization process.

1. Fully analytic bi-level

The simplest and most direct approach is to employ these analytic statistics and their design derivatives directly within an optimization loop. This approach is known as bi-level OUU, since there is an inner level uncertainty analysis nested within an outer level optimization.

Consider the common reliability-based design example of a deterministic objective function with a reliability constraint:

$$\begin{aligned} \text{minimize} \quad & f \\ \text{subject to} \quad & \beta \geq \bar{\beta} \end{aligned} \tag{52}$$

where β is computed relative to a prescribed threshold response value $\bar{z}$ and is constrained by a prescribed reliability level $\bar{\beta}$. Another common example is robust design in which the constraint enforcing a reliability lower-bound has been replaced with a constraint enforcing a variance upper-bound:

$$\begin{aligned} \text{minimize} \quad & f \\ \text{subject to} \quad & \sigma^2 \leq \bar{\sigma}^2 \end{aligned} \tag{53}$$

Solving these problems using a bi-level approach involves computing $\beta(\boldsymbol{s})$ and $\frac{d\beta}{d\boldsymbol{s}}$ for Eq. 52 or σ^2 and $\frac{d\sigma^2}{d\boldsymbol{s}}$ for Eq. 53 for each set of design variables $\boldsymbol{s}$ passed from the optimizer. This approach is explored for both uncertain and combined expansions using PCE and SC.

2. Sequential

An alternative OUU approach is the sequential approach, in which additional efficiency is sought through breaking the nested relationship of the UQ and optimization loops. The general concept is to iterate between optimization and uncertainty quantification, updating the optimization goals based on the most recent uncertainty assessment results. This approach is common with the reliability methods community, for which the updating strategy may be based on safety factors[29] or other approximations.[30]

A particularly effective approach for updating the optimization goals is to use data fit surrogate models, and in particular, local Taylor series models allow direct insertion of stochastic sensitivity analysis capabilities. In Ref. 10, first-order Taylor series approximations were explored, and in Ref. 11, second-order Taylor series approximations are investigated. In both cases, a trust-region model management framework[31] is used to adaptively manage the extent of the approximations and ensure convergence of the OUU process. Surrogate models are used for both the objective and the constraint functions, although the use of surrogates is only required for the functions containing statistical results; deterministic functions may remain explicit is desired.

In particular, trust-region surrogate-based optimization for reliability-based design employs surrogate models of f and β within a trust region Δ^k centered at $\mathbf{s}_c$:

$$\begin{aligned} \text{minimize} \quad & f(\mathbf{s}_c) + \nabla_s f(\mathbf{s}_c)^T(\mathbf{s} - \mathbf{s}_c) \\ \text{subject to} \quad & \beta(\mathbf{s}_c) + \nabla_s \beta(\mathbf{s}_c)^T(\mathbf{s} - \mathbf{s}_c) \geq \bar{\beta} \\ & \| \mathbf{s} - \mathbf{s}_c \|_\infty \leq \Delta^k \end{aligned} \tag{54}$$

and trust-region surrogate-based optimization for robust design employs surrogate models of f and σ^2 within a trust region Δ^k centered at $\mathbf{s}_c$:

$$\begin{array}{rc} \text{minimize} & f(\mathbf{s}_c) + \nabla_s f(\mathbf{s}_c)^T(\mathbf{s}-\mathbf{s}_c) \\ \text{subject to} & \sigma^2(\mathbf{s}_c) + \nabla_s \sigma^2(\mathbf{s}_c)^T(\mathbf{s}-\mathbf{s}_c) \leq \bar{\sigma}^2 \\ & \| \mathbf{s}-\mathbf{s}_c \|_\infty \leq \Delta^k \end{array} \tag{55}$$

Second-order local surrogates may also be employed, where the Hessians are typically approximated with quasi-Newton updates. The sequential approach will be explored for uncertain expansions using PCE and SC.

3. Multifidelity

The multifidelity OUU approach is another trust-region surrogate-based approach. Instead of the surrogate UQ model being a simple data fit (in particular, first-/second-order Taylor series model) of the truth UQ model results, we now employ distinct UQ models of differing fidelity. This differing UQ fidelity could stem from the fidelity of the underlying simulation model, the fidelity of the UQ algorithm, or both. In this paper, we focus on the fidelity of the UQ algorithm. For reliability-based multifidelity methods, this could entail varying fidelity in approximating assumptions (e.g., Mean Value for low fidelity, SORM for high fidelity),[11] and for stochastic expansion-based multifidelity methods, it could involve differences in selected levels of p and k refinement.

In this paper, we define UQ fidelity as point-wise accuracy in the design space and take the high fidelity truth model to be the uncertain expansion PCE/SC model, with validity only at a single design point. The low fidelity model, whose validity over the design space will be adaptively controlled, will be either the combined expansion PCE/SC model, with validity over a range of design parameters, or the Mean Value reliability method, with validity only at a single design point. The combined expansion low fidelity approach will span the current trust region of the design space and will be reconstructed for each new trust region. Trust region adaptation will ensure that the combined expansion approach remains sufficiently accurate for design purposes. By taking advantage of the design space spanning, we can reduce the cost of multiple low fidelity UQ analyses within the trust region, with fallback to the greater accuracy and higher expense of the uncertain expansion approach when needed. The Mean Value low fidelity approximation must be reformed for each change in design variables, but it only requires a single evaluation of a response function and its derivative for each UQ analysis. It is the least expensive UQ option, but its limited accuracy may dictate the use of small trust regions, resulting in greater iterations to convergence. The expense of optimizing a combined expansion, on the other hand, is not significantly less than that of optimizing the high fidelity UQ model, but its representation of global trends should allow the use of larger trust regions, resulting in reduced iterations to convergence. The design derivatives of each of the PCE/SC expansion models provide the necessary data to correct the low fidelity model to first-order consistency with the high fidelity model at the center of each trust region. Design derivatives of the Mean Value statistics are currently evaluated numerically using forward finite differences.

Multifidelity optimization for reliability-based design can be formulated as:

$$\begin{array}{rc} \text{minimize} & f(\mathbf{s}) \\ \text{subject to} & \hat{\beta_{hi}}(\mathbf{s}) \geq \bar{\beta} \\ & \| \mathbf{s}-\mathbf{s}_c \|_\infty \leq \Delta^k \end{array} \tag{56}$$

and multifidelity optimization for robust design can be formulated as:

$$\begin{array}{rc} \text{minimize} & f(\mathbf{s}) \\ \text{subject to} & \hat{\sigma_{hi}}^2(\mathbf{s}) \leq \bar{\sigma}^2 \\ & \| \mathbf{s}-\mathbf{s}_c \|_\infty \leq \Delta^k \end{array} \tag{57}$$

where the deterministic objective function is not approximated and $\hat{\beta_{hi}}$ and $\hat{\sigma_{hi}}^2$ are the approximated high-fidelity UQ results resulting from correction of the low-fidelity UQ results. In the case of an additive correction function:

$$\hat{\beta_{hi}}(\mathbf{s}) = \beta_{lo}(\mathbf{s}) + \alpha_\beta(\mathbf{s}) \tag{58}$$

$$\hat{\sigma_{hi}}^2(\mathbf{s}) = \sigma^2_{lo}(\mathbf{s}) + \alpha_{\sigma^2}(\mathbf{s}) \tag{59}$$

where correction functions $\alpha(\mathbf{s})$ enforcing first-order consistency[32] will be explored. Quasi-second-order correction functions[32] can also be explored, but care must be taken due to the different rates of curvature accumulation between the low and high fidelity models. In particular, since the low fidelity model is evaluated more frequently than the high fidelity model, it accumulates curvature information more quickly, such that enforcing quasi-second-order consistency with the high fidelity model can be detrimental in the initial iterations of the algorithm[d]. Instead, this consistency should only be enforced when sufficient high fidelity curvature information has been accumulated (e.g., after n rank one updates).

C. Epistemic Uncertainty Quantification

Given the capability to compute analytic statistics of the response along with design sensitivities of these statistics, we pursue optimization-based interval estimation approaches for mixed aleatory-epistemic uncertainty quantification. We first present the optimization interval estimation process, followed by two UQ approaches that may employ it.

Similar to the OUU approaches presented previously, we will employ derivatives of the statistics with respect to the nonprobabilistic parameters, where applicable, in order to guide optimization processes. But rather than performing a single minimization of an objective function subject to constraints, we will solve two related bound-constrained problems:

$$\begin{aligned} \text{minimize} \quad & M(s) \\ \text{subject to} \quad & s_L \leq s \leq s_U \end{aligned} \tag{60}$$

$$\begin{aligned} \text{maximize} \quad & M(s) \\ \text{subject to} \quad & s_L \leq s \leq s_U \end{aligned} \tag{61}$$

where $M(s)$ is a metric of interest, probabilistic in the general mixed uncertainty case and deterministic in the pure epistemic case. That is, in the general case of mixed aleatory and epistemic variables, we are computing an interval on a statistic of a response function (mean, variance, or CDF/CCDF ordinate/abscissa), and in the pure epistemic case (no aleatory uncertain variables), we are computing an interval on the response function itself.

At the interval estimation level, a key to computational efficiency is reusing as much information as possible within the solution procedures for these two related optimization problems. For gradient-based local approaches, we may only be able to reuse the evaluation of aleatory statistics and their derivatives at the initial epistemic point. For nongradient-based global approaches, however, we will make significant reuse of surrogate model interpolation (EGO) and box partitioning (DIRECT) data. In addition, the same OUU machinery for bi-level, sequential, and multifidelity approaches can be applied to reduce expense. At the aleatory UQ level, a key issue is again the use of combined variable expansions over both epistemic and aleatory parameters versus the use of expansions over only the aleatory parameters for each instance of the epistemic parameters. In this paper, we focus initially on bi-level nongradient-based global interval estimation employing combined and aleatory expansions.

1. Second-order probability

In second-order probability[33] (SOP), we segregate the aleatory and epistemic variables and perform nested iteration, with aleatory analysis on the inner loop and epistemic analysis on the outer loop. Starting from a specification of intervals and probability distributions on the inputs (as described in Section V.A.6, the intervals may augment the probability distributions, insert into the probability distributions, or some combination), we generate an ensemble of CDF/CCDF probabilistic results (a "horse tail"), one CDF/CCDF result for each aleatory analysis. Given that the ensemble stems from multiple realizations of the epistemic uncertainties, the interpretation is that each CDF/CCDF instance has no relative probability of occurrence, only that each instance is possible. For prescribed response levels on the CDF/CCDF, an interval on the probability is computed based on the bounds of the horse tail at that level, and vice versa for prescribed probability levels.

[d] Analytic and numerical Hessian data, when available, is instantaneous with no accumulation rate concerns.

2. Dempster-Schafer

In the Dempster-Schafer theory of evidence[33] (DSTE) approach, we start from a set of basic probability assignments (BPAs) for the epistemic uncertain variables, typically derived from a process of expert elicitation. These BPAs define sets of intervals for each epistemic variable, and for each possible combination of these intervals among the variables, we solve minimization and maximization problems for the interval of the response. These intervals define belief and plausibility functions that bound the true probability distribution of the response.

When aleatory uncertainties are also present, we may choose either to discretize the aleatory probability distributions into sets of intervals and treat them as well-characterized epistemic variables, or we may choose to segregate the aleatory uncertainties and treat them within an inner loop. In this latter case, DSTE can be seen as a generalization of SOP, in that the SOP interval minimization and maximization process is performed repeatedly for each "cell" defined by the BPAs in the DSTE analysis. As for SOP, this nested DSTE analysis reports intervals on statistics, and in particular, belief and plausibility results for statistics that are consistent with the epistemic evidence.

VI. Computational Results

Capabilities for uncertainty analysis and design based on nonintrusive polynomial chaos and stochastic collocation have been implemented in DAKOTA,[34] an open-source software framework for design and performance analysis of computational models on high performance computers. This section compares PCE and SC performance results for several algebraic benchmark test problems. These results build upon PCE results for UQ presented in Ref. 5, comparisons of PCE and SC results for UQ presented in Ref. 35, and PCE-based and SC-based optimization under uncertainty results presented in Ref. 36.

A. Lognormal ratio

This test problem has a limit state function (i.e., a critical response metric which defines the boundary between safe and failed regions of the random variable parameter space) defined by the ratio of two correlated, identically-distributed random variables.

$$g(\mathbf{x}) = \frac{x_1}{x_2} \tag{62}$$

The distributions for both x_1 and x_2 are Lognormal(1, 0.5) with a correlation coefficient between the two variables of 0.3. A nonlinear variable transformation is applied and Hermite orthogonal polynomials are employed in the transformed space.

1. Uncertainty quantification with PCE and SC

For the UQ analysis, 24 response levels (.4, .5, .55, .6, .65, .7, .75, .8, .85, .9, 1, 1.05, 1.15, 1.2, 1.25, 1.3, 1.35, 1.4, 1.5, 1.55, 1.6, 1.65, 1.7, and 1.75) are mapped into the corresponding cumulative probability levels. For this problem, an analytic solution is available and is used for comparison to CDFs generated from sampling on the chaos expansions using 10^6 samples.

Figure 4(a) compares tensor-product quadrature for traditional PCE (total-order expansion), tailored PCE (tensor-product expansion), and SC. It is evident for tensor-product quadrature that tailored PCE not only closes the performance gap between traditional PCE and SC, it completely eliminates it. In fact, a recent analysis[37] demonstrates that synchronized tensor-product PCE and SC can be proved identical for the tensor-product quadrature case. Finally, Figure 4(b) compares Smolyak sparse grids with linear and nonlinear growth rules for synchronized total-order PCE, heuristic total-order PCE, and SC. It is evident that tailored PCE is an improvement, but it still falls short of SC performance. This gap closes further with the use of linear growth rules that reduce computational effort spent resolving monomials that do not appear in the total-order expansion (i.e., monomials below the red line in Figure 3(b) versus those below the red line in Figure 3(a)).

B. Rosenbrock

The two-dimensional Rosenbrock function is a popular test problem for gradient-based optimization algorithms due to its difficulty for first-order methods. It turns out that this is also a challenging problem for

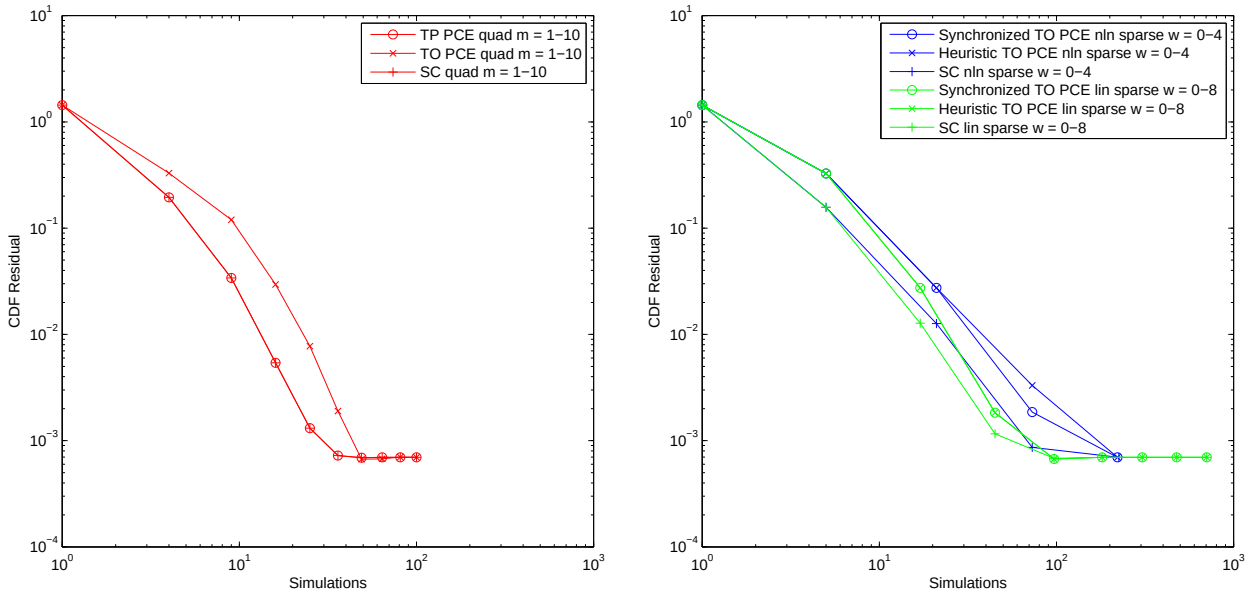

(a) Tensor-product quadrature.

(b) Smolyak sparse grids.

Figure 4. CDF residuals for lognormal ratio test problem evaluated with 10^6 samples: elimination of PCE/SC performance gap for TPQ and closing of performance gap for SSG.

certain UQ methods (especially local reliability methods), since a particular response level contour involves a highly nonlinear curve that may encircle the mean point (leading to multiple most probable points of failure). The function is a fourth order polynomial of the form:

$$f(x_1, x_2) = 100(x_2 - x_1^2)^2 + (1 - x_1)^2 \tag{63}$$

A three-dimensional plot of this function is shown in Figure 5(a), where both x_1 and x_2 range in value from -2 to 2. Figure 5(b) shows a contour plot for Rosenbrock's function where the encircling of a mean value at (0,0) is evident. Variables x_1 and x_2 are modeled as independent random variables using probability distributions selected from the Askey set: normal, uniform, exponential, beta, and gamma distributions. A linear variable transformation is used to account for scaling and Askey orthogonal polynomials are employed in the transformed space.

1. Uncertainty quantification with PCE and SC

For the UQ analysis, six response levels (.1, 1., 50., 100., 500., and 1000.) are mapped into the corresponding cumulative probability levels. Since analytic CDF solutions are not available for this problem, accuracy comparisons involve comparisons of statistics generated by sampling on the PCE approximation with statistics generated by sampling on the original response metric, where the sampling sets are of the same size and generated with the same random seed.

In Ref. 5, the expansion order is fixed at four and the exact coefficients are obtained for a quadrature order of five or greater, as expected for integrals (Eq. 15) involving a product of a fourth order function and fourth order expansion terms (refer to Section IV.A.2). Furthermore, with anisotropic quadrature and tensor-product expansions, the function can be integrated exactly with fifth order quadrature in x_1 and third order quadrature in x_2, reducing the expense from 25 simulations (isotropic) to only 15 simulations (anisotropic).

In Figure 6, the expansion order is again fixed at four, and we vary the distribution type and polynomial basis, including two standard normal variables using a Hermite basis, two uniform variables on $[-2, 2]$ using a Legendre basis, two exponential variables with $\beta = 2$ using a Laguerre basis, two beta variables with $\alpha = 1$ and $\beta = 0.5$ using a Jacobi basis, two gamma variables with $\alpha = 1.5$ and $\beta = 2$ using a generalized Laguerre basis, and five variables (normal, uniform, exponential, beta, and gamma with the same distribution parameters) using a mixed basis. For the mixed expansion over five variables, the standard two-dimensional

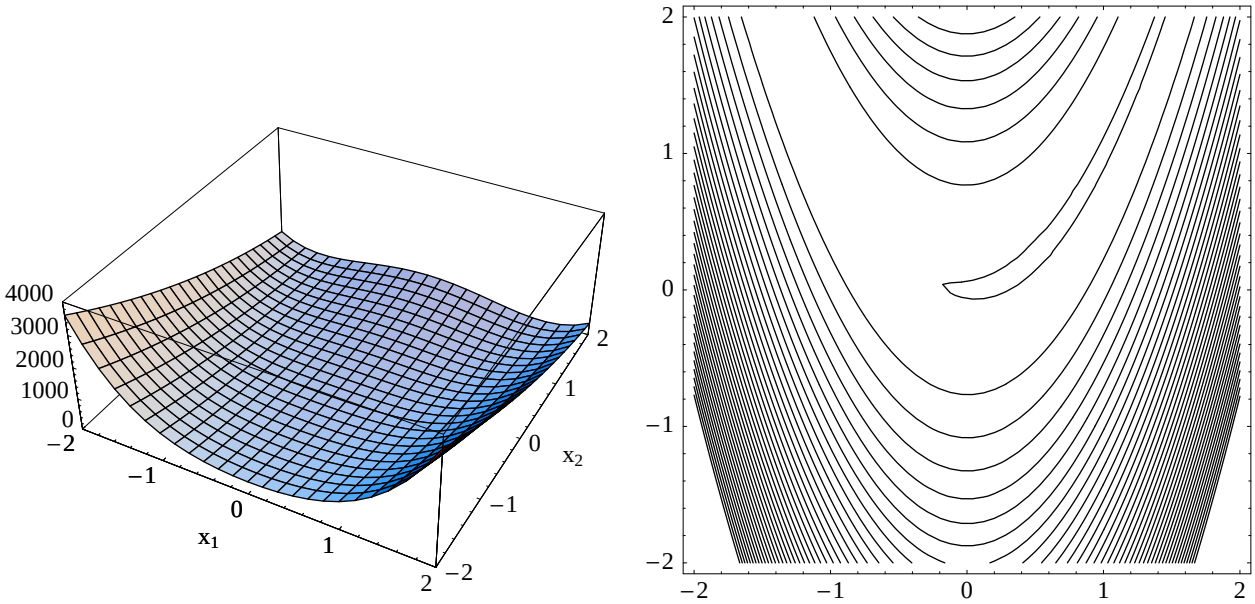

(a) 3-D plot. (b) Contours.

Figure 5. Rosenbrock's function.

Rosenbrock is generalized to n-dimensions as defined in Ref. 38. In all cases, a fourth-order expansion with sufficient integration is exact as expected, which provides verification of the Askey basis implementation. In

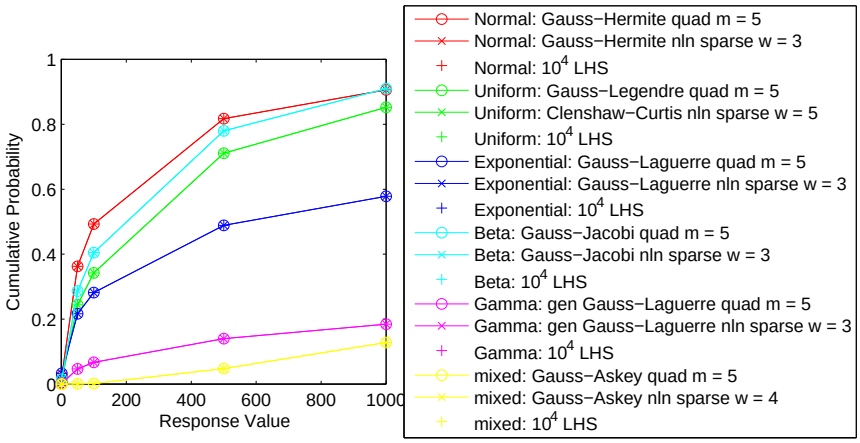

Figure 6. Varying distribution type, PCE basis, and integration approach for Rosenbrock test problem with fixed expansion order = 4.

Figure 7, we reperform the verification tests for SC and the expansion is again exact for sufficient quadrature and sparse grid integration levels.

For each tensor product quadrature (TPQ) case, fifth-order quadrature is used in combination with tailored tensor-product PCE and SC. Whereas the TPQ requirements are the same for PCE and SC, important differences are observed for Smolyak sparse grid (SSG) integrations with either linear or nonlinear growth rules. Tables 2 and 3 summarize the order/level requirements and the associated function evaluation counts, where non-nested rules include Gauss-Laguerre, Gauss-Jacobi, and generalized Gauss-Laguerre for exponential, beta, and gamma distributions; weakly-nested rules include Gauss-Hermite and Gauss-Legendre for normal and (anisotropic) uniform distributions; and fully-nested rules include Clenshaw-Curtis for (isotropic) uniform distributions.

For sparse grids with nonlinear growth rules, tailored total-order PCE is used and the two-variable

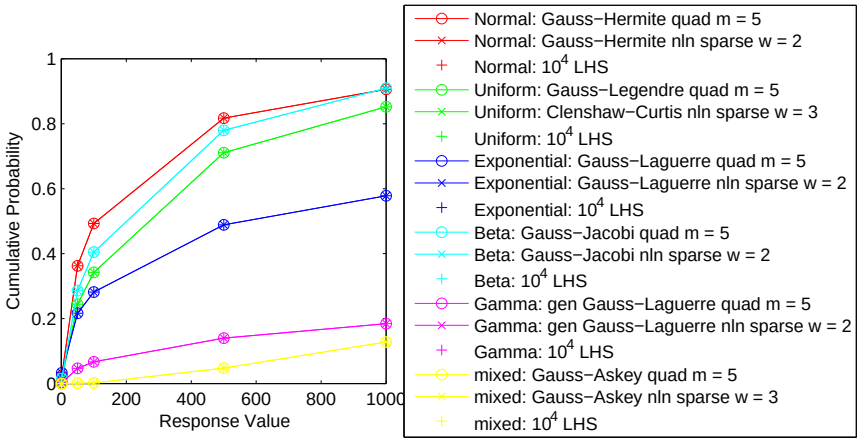

Figure 7. Varying distribution type and collocation point set for SC on the Rosenbrock test problem.

Table 2. PCE and SC expense for exact results in 2D Rosenbrock test problem.

UQ Approach	Integration Approach	Rule Nesting	Required Order/Level	Fn Evaluations
PCE	TPQ	Non	m = 5	25
PCE	Nonlinear SSG	Non	w = 3	95
PCE	Nonlinear SSG	Weak	w = 3	73
PCE	Nonlinear SSG	Full	w = 5	145
PCE	Linear SSG	Non	w = 3	63
PCE	Linear SSG	Weak	w = 3	45
SC	TPQ	Non	m = 5	25
SC	Nonlinear SSG	Non	w = 2	29
SC	Nonlinear SSG	Weak	w = 2	21
SC	Nonlinear SSG	Full	w = 3	29
SC	Linear SSG	Non	w = 2	25
SC	Linear SSG	Weak	w = 2	17

Table 3. PCE and SC expense for exact results in 5D Rosenbrock test problem.

UQ Approach	Integration Approach	Rule Nesting	Required Order/Level	Fn Evaluations
PCE	TPQ	Non	m = 5	3125
PCE	Nonlinear SSG	Non/Weak	w = 4	3579
PCE	Linear SSG	Non/Weak	w = 4	2273
SC	TPQ	Non	m = 5	3125
SC	Nonlinear SSG	Non/Weak	w = 3	700
SC	Linear SSG	Non/Weak	w = 2	104

Gaussian cases require level = 3, the fully-nested two-variable Clenshaw-Curtis case requires level = 5, and the five variable mixed Gaussian case requires level = 4 for exact results. SC obtains exact results with at least one lower level (level = 2 for two-dimensional Gaussian rules and level = 3 for both two-dimensional Clenshaw-Curtis and five-dimensional Gaussian). As shown in the tables, this corresponds to reductions in expense from 73 to 21 (2D weakly nested), 95 to 29 (2D non-nested), 145 to 29 (2D fully nested), and 3579 to 700 (5D weakly/non-nested) evaluations.

For linear sparse grid growth rules in Gaussian integrations (Clenshaw-Curtis cases retain nonlinear growth), exact integration in PCE requires level = 3 for the two-variable Gaussian cases and level = 4 for the five variable mixed Gaussian case. For SC, an exact Rosenbrock representation requires level = 2 for all cases. This corresponds to reductions in expense from 45 to 17 (2D weakly nested), 63 to 25 (2D non-nested), and 2273 to 104 (5D weakly/non-nested) evaluations, for SC linear SSG relative to PCE linear SSG. For SC linear SSG relative to SC nonlinear SSG, reductions are from 21 to 17 (2D weakly nested), 29 to 25 (2D non-nested), and 700 to 104 (5D weakly/non-nested) evaluations.

In two dimensions, TPQ and linear SSG are competitive (TPQ slightly better for PCE, SSG slightly better for SC), but with an increase to five dimensions, SSG demonstrates signficant benefits. Overall, SC with linear SSG is the top performer in both two and five dimensions.

2. Design under uncertainty

Since exact results can be obtained for Rosenbrock using stochastic expansions, a simple OUU formulation is demonstrated that provides exact results for both analytic design sensitivity formulations. Taking x_1 to be a design variable with initial value -0.75 and bounds $-2 \leq x_1 \leq 2$ and taking x_2 to be a standard normal random variable ($\mu = 0, \sigma = 1$), Table 4 shows the computational results for maximizing β_{cdf} for $\bar{z} = 10$. with either SC or fourth-order Hermite PCE and either Gauss-Hermite TPQ order = 5, Gauss-Hermite SSG level = 1 (uncertain expansions) with linear growth, or mixed Gauss-Hermite/Gauss-Legendre SSG level = 2 (combined expansions) with linear growth. Sequential results are shown for first-order and quasi-second-order Taylor series linkages and multifidelity results are shown for first-order additive corrections. Quasi-second-order formulations employ symmetric rank one (SR1) updates. For each of the multifidelity approaches, the "high fidelity" UQ model is the uncertain expansion approach, using the same settings as in its corresponding bi-level approach. The "low fidelity" UQ model is either the combined expansion approach, again using the same settings as in its corresponding bi-level approach, or a MVFOSM UQ analysis. For the bi-level approaches, the analytic sensitivity results are verified against results using finite difference sensitivities for the objective function. NPSOL's sequential quadratic programming (SQP) method is used as the optimizer.

For this problem, the functional input/output relationship can be captured exactly and all techniques are equally successful in locating the optimum at the lower bound of x_1. The only discernable difference in accuracy appears in the PCE bi-level SSG results (highlighted in red), for which it can be seen that the combined approach does not produce an accurate reliability index for SSG level = 2. Rather, SSG level = 3 (not shown) is required for this approach to generate the desired 2.091 value, at an increased cost of 45 function evaluations. SC, on the other hand, shows greater accuracy in generating the desired result at the lower SSG level in the corresponding bi-level combined formulation (highlighted in green).

For this low dimensional problem, SSG is already slightly less expensive than TPQ. As expected, the analytic-uncertain approach, relative to the analytic-combined approach, trades a reduction in simulation evaluations for a requirement of higher order information per simulation. Both the analytic-combined and the numerical-combined approaches form only a single expansion for which both moment and moment sensitivity evaluations for all design variable values involve only post-processing of the expansion. The sequential and multifidelity approaches require only a single trust region iteration to achieve hard convergence (Karush-Kuhn-Tucker optimality conditions satisfied), such that quasi-second-order linkages (which require at least two iterations to accumulate curvature information) provide no benefit. Overall, the sequential approaches employing linear SSG are the most efficient techniques for this problem (highlighted in blue), followed closely by the bi-level uncertain expansion approaches employing linear SSG (highlighted in magenta).

C. Short column

This test problem involves the plastic analysis of a short column with rectangular cross section (width $b = 5$ and depth $h = 15$) having uncertain material properties (yield stress Y) and subject to uncertain loads

Table 4. PCE-based and SC-based design results, Rosenbrock test problem.

OUU Approach	Sensitivity Approach	Expansion Variables	Integration Approach	Evaluations (Fn, Grad)	β
PCE Bi-level	Analytic	Uncertain	TPQ	(15, 15)	2.091
PCE Bi-level	Analytic	Combined	TPQ	(25, 0)	2.091
PCE Bi-level	Numerical	Uncertain	TPQ	(45, 0)	2.091
PCE Bi-level	Numerical	Combined	TPQ	(25, 0)	2.091
PCE Sequential 1	Analytic	Uncertain	TPQ	(15, 10)	2.091
PCE Sequential Q2	Analytic	Uncertain	TPQ	(15, 10)	2.091
PCE Multifid 1	Analytic	LF Comb, HF Unc	TPQ	(40, 10)	2.091
PCE/MV Multifid 1	LF Num, HF Ana	LF MV, HF Unc	TPQ	(20, 16)	2.091
PCE Bi-level	Analytic	Uncertain	Linear SSG	(9, 9)	2.091
PCE Bi-level	Analytic	Combined	Linear SSG	(17, 0)	1.641
PCE Bi-level	Numerical	Uncertain	Linear SSG	(27, 0)	2.091
PCE Bi-level	Numerical	Combined	Linear SSG	(17, 0)	1.641
PCE Sequential 1	Analytic	Uncertain	Linear SSG	(9, 6)	2.091
PCE Sequential Q2	Analytic	Uncertain	Linear SSG	(9, 6)	2.091
PCE Multifid 1	Analytic	LF Comb, HF Unc	Linear SSG	(49, 9)	2.091
PCE/MV Multifid 1	LF Num, HF Ana	LF MV, HF Unc	Linear SSG	(14, 12)	2.091
SC Bi-level	Analytic	Uncertain	TPQ	(15, 15)	2.091
SC Bi-level	Analytic	Combined	TPQ	(25, 0)	2.091
SC Bi-level	Numerical	Uncertain	TPQ	(45, 0)	2.091
SC Bi-level	Numerical	Combined	TPQ	(25, 0)	2.091
SC Sequential 1	Analytic	Uncertain	TPQ	(15, 10)	2.091
SC Sequential Q2	Analytic	Uncertain	TPQ	(15, 10)	2.091
SC Multifid	Analytic	LF Comb, HF Unc	TPQ	(40, 10)	2.091
SC/MV Multifid 1	LF Num, HF Ana	LF MV, HF Unc	TPQ	(20, 16)	2.091
SC Bi-level	Analytic	Uncertain	Linear SSG	(9, 9)	2.091
SC Bi-level	Analytic	Combined	Linear SSG	(17, 0)	2.091
SC Bi-level	Numerical	Uncertain	Linear SSG	(27, 0)	2.091
SC Bi-level	Numerical	Combined	Linear SSG	(17, 0)	2.091
SC Sequential 1	Analytic	Uncertain	Linear SSG	(9, 6)	2.091
SC Sequential Q2	Analytic	Uncertain	Linear SSG	(9, 6)	2.091
SC Multifid 1	Analytic	LF Comb, HF Unc	Linear SSG	(26, 6)	2.091
SC/MV Multifid 1	LF Num, HF Ana	LF MV, HF Unc	Linear SSG	(14, 12)	2.091

(bending moment M and axial force P).[39] The limit state function is defined as:

$$g(\mathbf{x}) = 1 - \frac{4M}{bh^2Y} - \frac{P^2}{b^2h^2Y^2} \tag{64}$$

The distributions for P, M, and Y are Normal(500, 100), Normal(2000, 400), and Lognormal(5, 0.5), respectively, with a correlation coefficient of 0.5 between P and M (uncorrelated otherwise). A nonlinear variable transformation is applied and Hermite orthogonal polynomials are employed in the transformed space.

1. Uncertainty quantification with PCE and SC

Figure 8 shows convergence of the mean and standard deviation of the limit state function for increasing quadrature orders and linear/nonlinear sparse grid levels using tailored PCE, traditional PCE, and SC. Since an analytic solution is not available, residuals are measured relative to an "overkill" solution. The quality of this overkill solution and the effect of compounded round-off errors can be seen to hinder the convergence trajectories at residual values below 10^{-10} (short of double precision machine epsilon). point short of double In Figure 8(a), the only discernible differences appear among the set of tensor-product quadrature (TPQ) results, the set of linear Smolyak sparse grids (SSG) results, and the set of nonlinear SSG results, with similar performance among the three sets. In Figures 8(b,c), however, significant differences are evident. First, for TPQ (Figure 8(b)), tensor-product PCE (tailored) is again shown to completely eliminate the performance gap between total-order PCE (traditional) and SC. For SSG with nonlinear growth rules (Figure 8(c), blue lines), the heuristic total-order PCE approach (traditional) is shown to be nonconservative in its estimation of the order of expansion to employ. Through inclusion of monomials that exceed the order of what can be resolved, the expansion standard deviation fails to converge. The synchronized total-order PCE approach (tailored) is shown to be much more rigorous for nonlinear growth, although its performance falls well short of that of SC with nonlinear growth. Without this rigorous estimation, however, one would be left with the undesirable alternative of trial and error in synchronizing a nonlinear SSG with a PCE expansion order. For SSG with linear growth rules (Figure 8(c), green lines), improved heuristics are available and the synchronized and heuristic total-order PCE approaches can be seen to be identical. Thus, in the linear case, rigorous estimation of the set of nondominated monomials is not required. Further, while the performance gap with SC remains, its magnitude has been reduced relative to the gap in the nonlinear SSG case. Whereas TPQ outperforms linear/nonlinear SSG for the two-dimensional problem in Figure 4 (such that the equivalent tailored PCE and SC TPQ approaches performed the best), this trend has started to reverse with the increase to three dimensions and SC with linear SSG stands alone as the most rapidly converging technique.

2. Design under uncertainty

An objective function of cross-sectional area and a target reliability index of 2.5 are used in the design problem:

$$\begin{aligned} \min \quad & bh \\ \text{s.t.} \quad & \beta \geq 2.5 \\ & 5.0 \leq b \leq 15.0 \\ & 15.0 \leq h \leq 25.0 \end{aligned} \tag{65}$$

The initial design of $(b, h) = (5, 15)$ is infeasible and the optimization must add material to obtain the target reliability at the optimal design $(b, h) = (8.1147, 25.000)$ with an area of 202.87.

For PCE, Hermite expansions are again used, although in order to scale better for a slightly higher dimensional problem, tensor-product quadrature is replaced with point collocation using second-order uncertain expansions or third-order combined expansions with a factor of two oversampling (20 simulations per second-order uncertain expansion over three variables and 112 simulations per third-order combined expansion over five variables). For SC, point collocation is not available and tensor-product quadrature is retained with order = 3 for second-order uncertain expansions and order = 4 for third-order combined expansions, at considerable expense. Both PCE and SC are also explored with Smolyak sparse grids at level = 2 for second-order uncertain expansions and level = 3 for third-order combined expansions. NPSOL SQP method is again used as the optimizer, SR1 updates are used for quasi-second-order linkages in sequential approaches,

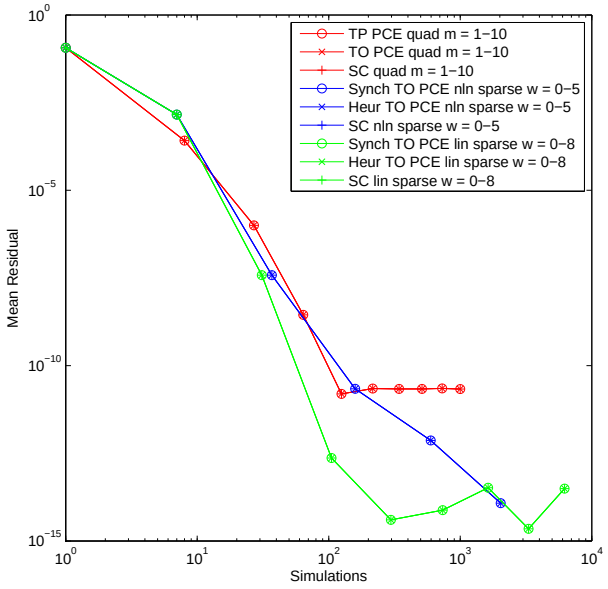

(a) Mean residual (TPQ and SSG).

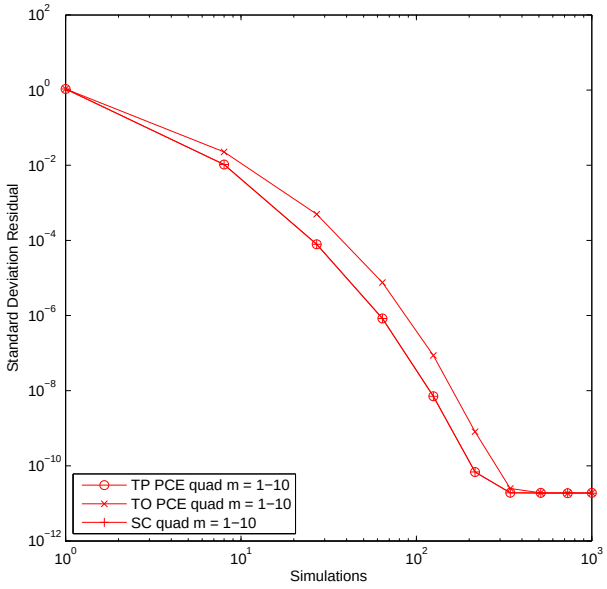

(b) Standard deviation residual (TPQ).

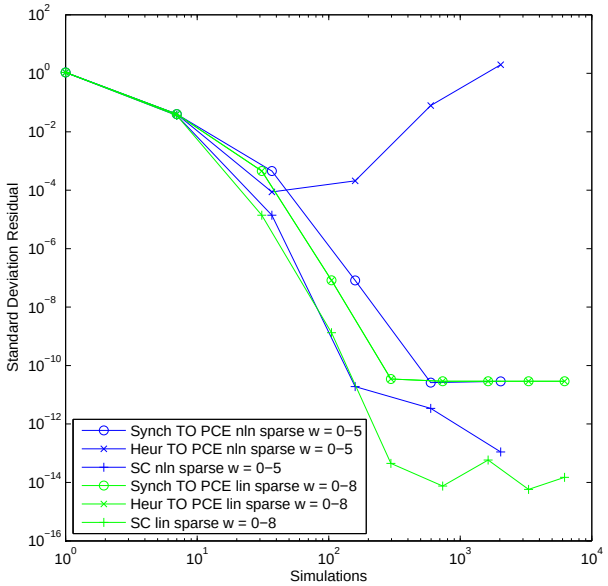

(c) Standard deviation residual (SSG).

Figure 8. Convergence of mean and standard deviation for the short column test problem.

and multifidelity approaches employ uncertain expansions as the high fidelity models and either combined expansions or MVFOSM as the low fidelity models (expansion approaches mirror the corresponding bi-level settings). Table 5 shows the computational results. As for the Rosenbrock OUU problem, the analytic sensitivity results for the bi-level methods are verified against results using numerical derivatives, although these results are omitted from this and all subsequent tables for brevity. For this problem, the functional in-

Table 5. PCE-based and SC-based design results, short column test problem.

OUU Approach	Sensitivity Approach	Expansion Variables	Integration Approach	Evaluations (Fn, Grad)	Area	β
PCE Bi-level	Analytic	Uncertain	Pt Colloc	(140, 60)	202.38	2.5001
PCE Bi-level	Analytic	Combined	Pt Colloc	(112, 0)	206.12	2.4998
PCE Sequential 1	Analytic	Uncertain	Pt Colloc	(240, 120)	202.39	2.5000
PCE Sequential Q2	Analytic	Uncertain	Pt Colloc	(220, 120)	202.39	2.5000
PCE Multifid 1	Analytic	LF Comb, HF Unc	Pt Colloc	(576, 120)	202.39	2.5000
PCE/MV Multifid 1	LF Num, HF Ana	LF MV, HF Unc	Pt Colloc	(204, 144)	202.39	2.5000
PCE Bi-level	Analytic	Uncertain	Linear SSG	(217, 93)	202.85	2.5001
PCE Bi-level	Analytic	Combined	Linear SSG	(341, 0)	200.47	2.5003
PCE Sequential 1	Analytic	Uncertain	Linear SSG	(372, 186)	202.85	2.5000
PCE Sequential Q2	Analytic	Uncertain	Linear SSG	(341, 186)	202.85	2.5000
PCE Multifid 1	Analytic	LF Comb, HF Unc	Linear SSG	(1333, 155)	202.85	2.5000
PCE/MV Multifid 1	LF Num, HF Ana	LF MV, HF Unc	Linear SSG	(281, 188)	202.85	2.5000
SC Bi-level	Analytic	Uncertain	TPQ	(189, 81)	202.86	2.5001
SC Bi-level	Analytic	Combined	TPQ	(1024, 0)	202.62	2.5002
SC Sequential 1	Analytic	Uncertain	TPQ	(324, 162)	202.86	2.5000
SC Sequential Q2	Analytic	Uncertain	TPQ	(297, 162)	202.86	2.5000
SC Multifid 1	Analytic	LF Comb, HF Unc	TPQ	(3288, 108)	202.86	2.5000
SC/MV Multifid 1	LF Num, HF Ana	LF MV, HF Unc	TPQ	(253, 172)	202.86	2.5000
SC Bi-level	Analytic	Uncertain	Linear SSG	(217, 93)	202.87	2.5001
SC Bi-level	Analytic	Combined	Linear SSG	(341, 0)	199.46	2.5001
SC Sequential 1	Analytic	Uncertain	Linear SSG	(372, 186)	202.86	2.5000
SC Sequential Q2	Analytic	Uncertain	Linear SSG	(341, 186)	202.86	2.5000
SC Multifid 1	Analytic	LF Comb, HF Unc	Linear SSG	(1333, 155)	202.86	2.5000
SC/MV Multifid 1	LF Num, HF Ana	LF MV, HF Unc	Linear SSG	(281, 188)	202.86	2.5000

put/output relationship is not captured exactly by the PCE and SC expansions (as it can be for Rosenbrock) and performance differences are more readily evident. For PCE-based approaches, the combined expansion results are less expensive to obtain, since they employ only a single expansion for all design variable sets, but these optima (highlighted in red) are approximate and the uncertain expansion approaches (highlighted in green) can be seen to converge more accurately. Under order/level refinement (not shown), the optima from the bi-level combined expansion approaches eventually converge to the optima from the uncertain expansion approaches; however, it is expensive: PCE and SC combined expansions with linear SSG require level = 6 at a cost of 13683 evaluations. Since the sequential approach takes more than a single iteration to converge, benefit from quasi-second-order linkage (highlighted in blue) is evident: accumulated curvature information converges the sequential iteration more quickly. In addition, the multifidelity machinery converges to the high fidelity result based on uncertain expansions despite the optimizer being interfaced only with the low fidelity combined expansion or MVFOSM UQ analyses. Overall, bi-level uncertain expansion approaches (highlighted in green) provide the most efficient and accurate techniques for this problem, followed by MV-based multifidelity approaches (highlighted in magenta), followed by quasi-second-order sequential approaches (highlighted in blue).

3. Epistemic interval estimation

As for the design problem in Eq. 65, we will study the cross-sectional area and reliability index. However, rather than optimizing the area subject to a constraint on the reliability, we will determine the output interval in these metrics resulting from epistemic uncertainties, where the epistemic variables are taken to be the beam width and depth (previously the design variables) with intervals of [5.0, 15.] and [15., 25.], respectively. The optimizer is the nongradient-based EGO algorithm, based on successive refinement of Gaussian process surrogate models. Smolyak sparse grids (SSG) with linear growth rules are employed for tailored total-order PCE and SC with aleatory and combined expansions, and point collocation (PC) is employed for total-order PCE with an oversampling ratio of two. Table 6 shows the results for a convergence study with increasing SSG levels for PCE and SC and increasing PC expansion orders for PCE compared to nested Latin hypercube sampling. It is evident that the PCE/SC aleatory expansion results using SSG converge by w = 3 (highlighted

Table 6. PCE-based and SC-based interval estimation results, short column test problem.

Interv Est Approach	UQ Approach	Expansion Variables	Evaluations (Fn, Grad)	Area	β
EGO	PCE SSG w = 2	Aleatory	(527, 0)	[75.0002, 374.999]	[-2.18824, 11.5924]
EGO	PCE SSG w = 3	Aleatory	(1785, 0)	[75.0002, 374.999]	[-2.18732, 11.5900]
EGO	PCE SSG w = 4	Aleatory	(5049, 0)	[75.0002, 374.999]	[-2.18732, 11.5900]
EGO	PCE PC p = 2	Aleatory	(340, 0)	[75.0002, 374.999]	[-2.20948, 11.6633]
EGO	PCE PC p = 3	Aleatory	(800, 0)	[75.0002, 374.999]	[-2.19030, 11.6002]
EGO	PCE PC p = 4	Aleatory	(1190, 0)	[75.0002, 374.999]	[-2.18737, 11.5904]
EGO	PCE SSG w = 4	Combined	(1341, 0)	[75.0002, 374.999]	[-2.31709, 17.6164]
EGO	PCE SSG w = 6	Combined	(13683, 0)	[75.0002, 374.999]	[-2.18969, 11.6939]
EGO	PCE SSG w = 8	Combined	(94473, 0)	[75.0002, 374.999]	[-2.18734, 11.5910]
EGO	PCE PC p = 4	Combined	(420, 0)	[75.0002, 374.999]	[-2.39482, 12.7956]
EGO	PCE PC p = 6	Combined	(924, 0)	[75.0002, 374.999]	[-2.20142, 12.6489]
EGO	PCE PC p = 8	Combined	(2574, 0)	[75.0002, 374.999]	[-2.19368, 11.5869]
EGO	SC SSG w = 2	Aleatory	(527, 0)	[75.0002, 374.999]	[-2.18735, 11.5900]
EGO	SC SSG w = 3	Aleatory	(1785, 0)	[75.0002, 374.999]	[-2.18732, 11.5900]
EGO	SC SSG w = 4	Aleatory	(5049, 0)	[75.0002, 374.999]	[-2.18732, 11.5900]
EGO	SC SSG w = 4	Combined	(1341, 0)	[75.0002, 374.999]	[-2.23439, 12.3640]
EGO	SC SSG w = 6	Combined	(13683, 0)	[75.0002, 374.999]	[-2.18804, 11.6002]
EGO	SC SSG w = 8	Combined	(94473, 0)	[75.0002, 374.999]	[-2.18732, 11.5901]
LHS 100	LHS 100	N/A	(10^4, 0)	[80.5075, 338.607]	[-2.14505, 8.64891]
LHS 1000	LHS 1000	N/A	(10^6, 0)	[76.5939, 368.225]	[-2.19883, 11.2353]
LHS 10^4	LHS 10^4	N/A	(10^8, 0)	[76.4755, 373.935]	[-2.16323, 11.5593]

in red) with an area interval of $[75., 375.]$ and a β interval of $[-2.18732, 11.5900]$. The PCE/SC combined expansion results using SSG also converge, although more slowly; by w = 8 (highlighted in green), the PCE results are accurate only to four digits and the SC results are only accurate to five digits. SC consistently outperforms PCE for this problem and numerical integration (SSG) generally provides more accurate results than regression (PC), such that the SC SSG aleatory expansion approach is the best performer, converging to five digits of accuracy by w = 2 at an expense of 527 evaluations (highlighted in blue). The nested sampling results are also converging to the correct intervals, although the results are only accurate to one or two digits for the area interval and two or three digits for the reliability index interval after 10^8 samples (highlighted in magenta).

D. Cantilever beam

The next test problem involves the simple uniform cantilever beam[29,40] shown in Figure 9. Random variables

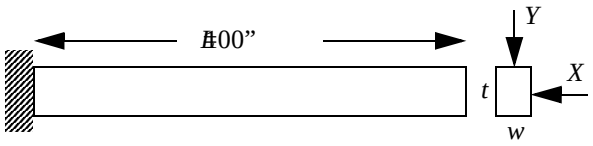

Figure 9. Cantilever beam test problem.

in the problem include the yield stress R and Youngs modulus E of the beam material and the horizontal and vertical loads, X and Y, which are modeled with normal distributions using N(40000, 2000), N(2.9E7, 1.45E6), N(500, 100), and N(1000, 100), respectively. Problem constants include $L = 100$ in. and $D_0 = 2.2535$ in. The beam response metrics have the following analytic form:

$$\text{stress} = \frac{600}{wt^2}Y + \frac{600}{w^2t}X \leq R \tag{66}$$

$$\text{displacement} = \frac{4L^3}{Ewt}\sqrt{(\frac{Y}{t^2})^2 + (\frac{X}{w^2})^2} \leq D_0 \tag{67}$$

These stress and displacement response functions are scaled using $\frac{\text{stress}}{R} - 1$ and $\frac{\text{displacement}}{D_0} - 1$, such that negative values indicate safe regions of the parameter space. A linear variable transformation is used to account for scaling of the normal PDFs and Hermite orthogonal polynomials are employed in the transformed space.

1. *Uncertainty quantification with PCE and SC*

Figure 10 shows convergence of the mean residuals and Figure 11 shows convergence of the standard deviation residuals for scaled stress and displacement for increasing quadrature orders and sparse grid levels using tailored PCE, traditional PCE, and SC. An analytic solution is again unavailable, so residuals are measured relative to an “overkill” solution such that convergence again slows at residual values below 10^{-10}.

In Figure 10, the only discernible difference appears between the sets of TPQ, linear SSG, and nonlinear

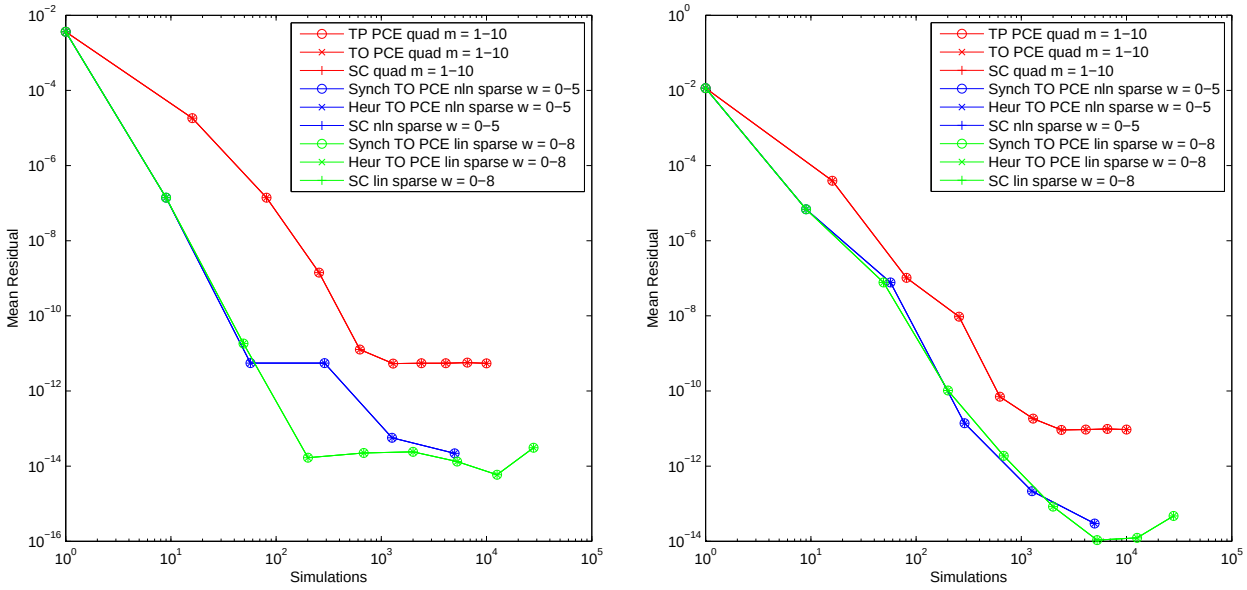

(a) Scaled stress (TPQ and SSG).

(b) Scaled displacement (TPQ and SSG).

Figure 10. Convergence of mean for PCE and SC in the cantilever beam test problem.

SSG results, with linear/nonlinear SSG outperforming TPQ for this four-dimensional problem. In Figure 11,

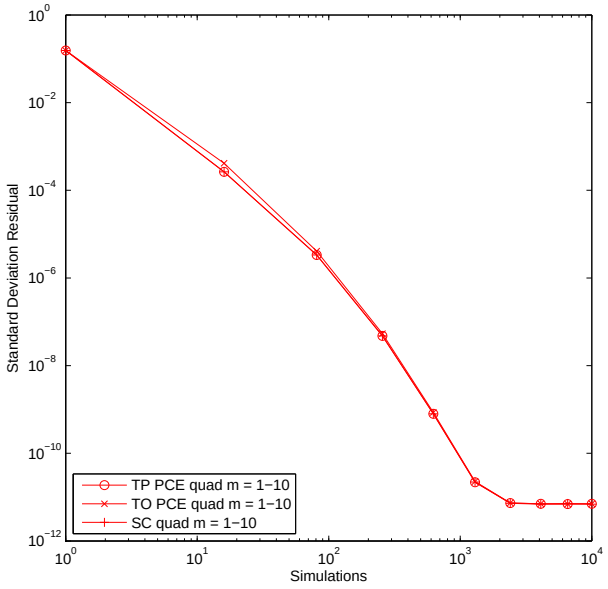

(a) Scaled stress (TPQ).

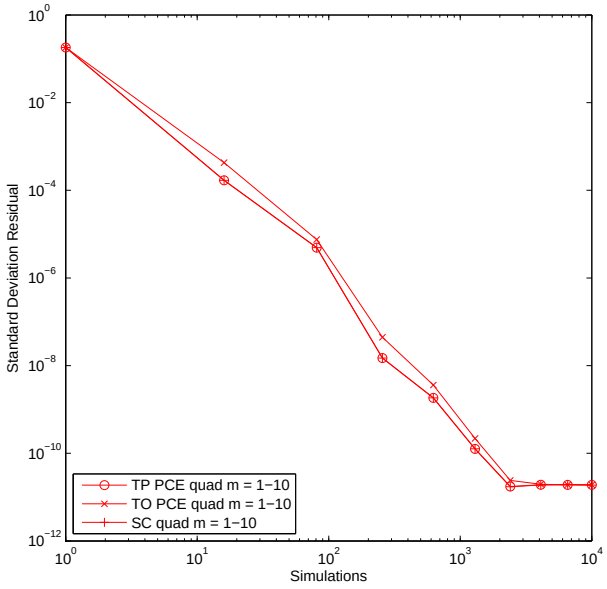

(b) Scaled displacement (TPQ).

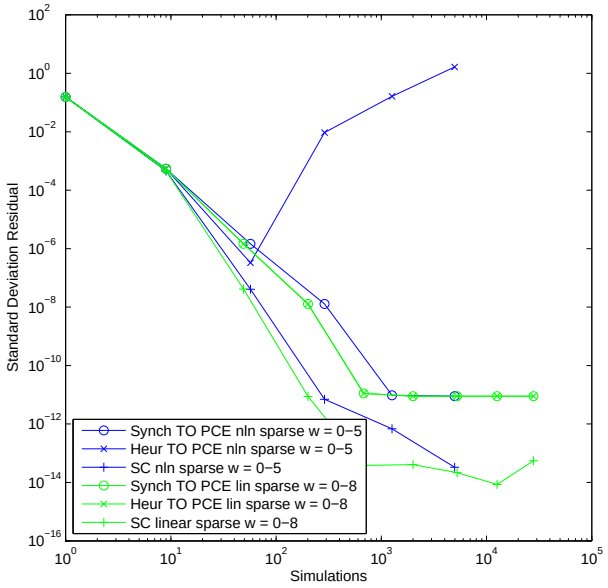

(c) Scaled stress (SSG).

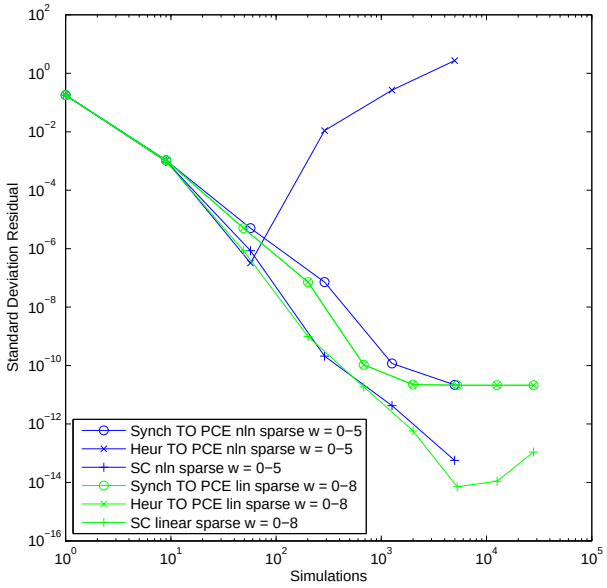

(d) Scaled displacement (SSG).

Figure 11. Convergence of standard deviation for PCE and SC in the cantilever beam test problem.

additional differences are again evident. For TPQ, the performance gap between total-order PCE (traditional) and SC is relatively small, but tensor-product PCE (tailored) is again shown to completely eliminate it. For nonlinear SSG (blue lines), the heuristic total-order PCE approach (traditional) is again shown to be nonconservative in its estimation of the order of expansion to employ, and the synchronized total-order PCE approach (tailored) is shown to be more rigorous, although it again falls short of the performance of SC. For linear SSG (green lines), synchronized and heuristic total-order PCE approaches are again identical and, while the performance gap with SC remains, its magnitude has been reduced relative to the gap in the nonlinear SSG case. As for the previous three-dimensional problem (Figure 8(b)), SC with linear SSG stands alone as the most efficient technique.

2. Design under uncertainty

The design problem is to minimize the weight (or, equivalently, the cross-sectional area) of the beam subject to the displacement and stress constraints. When seeking a 3-sigma reliability level (where reliability index β is based on moment projection) on these constraints, the design problem can be summarized as follows:

$$\begin{aligned} \min \quad & wt \\ \text{s.t.} \quad & \beta_S \geq 3.0 \\ & \beta_D \geq 3.0 \\ & 1.0 \leq w \leq 4.0 \\ & 1.0 \leq t \leq 4.0 \end{aligned} \tag{68}$$

For PCE, Hermite expansions are employed using either point collocation with second-order expansions and a factor of two oversampling (30 simulations per uncertain expansion over four variables and 56 simulations per combined expansion over six variables) or Smolyak sparse grids with level = 2 for uncertain expansions (which corresponds to a second-order expansion for tailored total-order PCE) and level = 4 for combined expansions (which corresponds to a fourth-order expansion). For SC, tensor-product quadrature with order = 3 or Smolyak sparse grids with level = 2 (uncertain) or level = 4 (combined) are employed. Again, NPSOL SQP is the optimizer, SR1 updates provide quasi-second-order linkages in sequential approaches, multifidelity approaches employ uncertain expansions as the high fidelity models and either combined expansions or MVFOSM as the low fidelity models (expansion approaches mirror the corresponding bi-level settings). Table 7 shows the computational results, where the fully converged optimal solution is $(w, t) = (2.434, 3.866)$ with area = 9.412, $\beta_S = 3.000$, and $\beta_D = 3.048$. For this problem, the functional input/output relationship is captured accurately enough by second-order uncertain expansions to converge to the correct solution. The combined expansion results, while again more affordable in most cases, do not have sufficient accuracy to locate the correct solution for either PCE or SC. The first-order sequential approaches also fail to converge for PCE and SC, whereas accumulation of curvature information mitigates this problem in each of these cases. The multifidelity approaches are successful in forcing the low fidelity results toward the high fidelity optima, with more accurate results obtained using Mean Value as the low fidelity model than for using combined PCE/SC expansions. Overall, the PCE Mean Value-based multifidelity approach with point collocation (highlighted in red) provides the most efficient technique for this problem, followed by the PCE bi-level uncertain expansion approach with point collocation (highlighted in green) and the slightly more accurate PCE/SC Mean Value-based multifidelity approaches with linear SSG (highlighted in blue).

3. Epistemic interval estimation

As for the design problem in Eq. 68, we will study the cross-sectional area and reliability indices of displacement and stress. However, rather than optimizing an objective subject to constraints, we will determine the output interval in these metrics resulting from epistemic uncertainties, where the epistemic variables are taken to be the beam width and thickness (previously the design variables) with intervals of [1.0, 10.]. The optimizer is the nongradient-based EGO algorithm, based on successive refinement of Gaussian process surrogate models. Smolyak sparse grids (SSG) with linear growth rules are employed for tailored total-order PCE and SC with aleatory and combined expansions, and point collocation (PC) is employed for total-order PCE with an oversampling ratio of two. Table 8 shows the results for a convergence study with increasing SSG levels for PCE and SC and increasing PC expansion orders for PCE compared to nested Latin hypercube sampling. It is evident that the PCE/SC aleatory expansion results using SSG converge by w = 3

Table 7. PCE-based and SC-based design results, cantilever beam test problem.

OUU Approach	Sensitivity Approach	Expansion Variables	Integration Approach	Evaluations (Fn, Grad)	Area	β_S	β_D
PCE Bi-level	Analytic	Uncertain	Pt Colloc	(330, 330)	9.410	3.000	3.033
PCE Bi-level	Analytic	Combined	Pt Colloc	(56, 0)	45.29	1.952	1.177
PCE Sequential 1	Analytic	Uncertain	Pt Colloc	(1050, 510)	4.198	-7.169	-8.332
PCE Sequential Q2	Analytic	Uncertain	Pt Colloc	(810, 420)	9.410	3.000	3.033
PCE Multifid 1	Analytic	LF Comb, HF Unc	Pt Colloc	(696, 180)	9.378	2.537	2.625
PCE/MV Multifid 1	LF Num, HF Ana	LF MV, HF Unc	Pt Colloc	(198, 138)	9.410	3.000	3.033
PCE Bi-level	Analytic	Uncertain	Linear SSG	(539, 539)	9.412	3.000	3.048
PCE Bi-level	Analytic	Combined	Linear SSG	(2381, 0)	9.327	3.000	3.000
PCE Sequential 1	Analytic	Uncertain	Linear SSG	(1617, 784)	4.192	-7.162	-8.318
PCE Sequential Q2	Analytic	Uncertain	Linear SSG	(833, 441)	9.412	3.000	3.048
PCE Multifid 1	Analytic	LF Comb, HF Unc	Linear SSG	(9916, 196)	9.420	3.002	3.495
PCE/MV Multifid 1	LF Num, HF Ana	LF MV, HF Unc	Linear SSG	(375, 231)	9.412	3.000	3.048
SC Bi-level	Analytic	Uncertain	TPQ	(891, 891)	9.411	3.000	3.048
SC Bi-level	Analytic	Combined	TPQ	(729, 0)	6.543	7.982	3.000
SC Sequential 1	Analytic	Uncertain	TPQ	(2673, 1296)	4.192	-7.162	-8.318
SC Sequential Q2	Analytic	Uncertain	TPQ	(2187, 1134)	9.411	3.000	3.048
SC Multifid 1	Analytic	LF Comb, HF Unc	TPQ	(9720, 810)	9.097	2.301	2.926
SC/MV Multifid 1	LF Num, HF Ana	LF MV, HF Unc	TPQ	(567, 327)	9.411	3.000	3.048
SC Bi-level	Analytic	Uncertain	Linear SSG	(539, 539)	9.412	3.000	3.048
SC Bi-level	Analytic	Combined	Linear SSG	(2381, 0)	8.932	3.000	5.347
SC Sequential 1	Analytic	Uncertain	Linear SSG	(1617, 784)	4.192	-7.161	-8.318
SC Sequential Q2	Analytic	Uncertain	Linear SSG	(833, 441)	9.412	3.000	3.048
SC Multifid 1	Analytic	LF Comb, HF Unc	Linear SSG	(10112, 294)	9.424	3.015	3.414
SC/MV Multifid 1	LF Num, HF Ana	LF MV, HF Unc	Linear SSG	(375, 231)	9.412	3.000	3.048

Table 8. PCE-based and SC-based interval estimation results, cantilever beam test problem.

Interv Est Approach	UQ Approach	Expansion Variables	Evaluations (Fn, Grad)	Area	β_S	β_D
EGO	PCE SSG w=2	Aleatory	(2646, 0)	[1.00002, 99.9998]	[-8.99220, 404.967]	[-9.63475, 1409.61]
EGO	PCE SSG w=3	Aleatory	(10854, 0)	[1.00002, 99.9998]	[-8.99211, 404.963]	[-9.63448, 1409.57]
EGO	PCE SSG w=4	Aleatory	(36774, 0)	[1.00002, 99.9998]	[-8.99211, 404.963]	[-9.63448, 1409.57]
EGO	PCE PC p=2	Aleatory	(1620, 0)	[1.00002, 99.9998]	[-9.64971, 405.456]	[-9.64971, 1411.77]
EGO	PCE PC p=3	Aleatory	(4200, 0)	[1.00002, 99.9998]	[-8.99173, 404.951]	[-9.63621, 1409.84]
EGO	PCE PC p=4	Aleatory	(7560, 0)	[1.00002, 99.9998]	[-8.99215, 404.964]	[-9.63389, 1409.48]
EGO	PCE SSG w=4	Combined	(2381, 0)	[1.00002, 99.9998]	[-12.0227, 28.4165]	[-12.8208, 13.9021]
EGO	PCE SSG w=6	Combined	(30869, 0)	[1.00002, 99.9998]	[-9.83782, 223.547]	[-10.9817, 60.0065]
EGO	PCE SSG w=8	Combined	(266489, 0)	[1.00002, 99.9998]	[-9.11001, 262.701]	[-9.95681, 160.428]
EGO	PCE PC p=4	Combined	(420, 0)	[1.00002, 99.9998]	[-8.56990, 4.40084]	[-4.83674, 1.22575]
EGO	PCE PC p=6	Combined	(1848, 0)	[1.00002, 99.9998]	[-7.59913, 3.43619]	[-5.85474, 0.997092]
EGO	PCE PC p=8	Combined	(6006, 0)	[1.00002, 99.9998]	[-7.04090, 2.36795]	[-3.98613, 0.464266]
EGO	SC SSG w=2	Aleatory	(2646, 0)	[1.00002, 99.9998]	[-8.99211, 404.962]	[-9.63453, 1409.56]
EGO	SC SSG w=3	Aleatory	(10854, 0)	[1.00002, 99.9998]	[-8.99211, 404.962]	[-9.63448, 1409.55]
EGO	SC SSG w=4	Aleatory	(36774, 0)	[1.00002, 99.9998]	[-8.99211, 404.962]	[-9.63448, 1409.56]
EGO	SC SSG w=4	Combined	(2381, 0)	[1.00002, 99.9998]	[-1.26801, ∞]	[-1.95236, ∞]
EGO	SC SSG w=6	Combined	(30869, 0)	[1.00002, 99.9998]	[-10.0003, ∞]	[-2.25563, ∞]
EGO	SC SSG w=8	Combined	(266489, 0)	[1.00002, 99.9998]	[-9.14279, 1479.76]	[-2.23834, ∞]
LHS 100	LHS 100	N/A	(10^4, 0)	[1.69100, 88.0090]	[-8.31258, 324.114]	[-9.34799, 1119.22]
LHS 1000	LHS 1000	N/A	(10^6, 0)	[1.18837, 96.1182]	[-8.85165, 381.884]	[-9.55299, 1304.75]
LHS 10^4	LHS 10^4	N/A	(10^8, 0)	[1.11023, 98.8855]	[-8.96612, 398.167]	[-9.59256, 1376.45]

(highlighted in red) with an area interval of $[1., 100.]$, a β_S interval of $[-8.9921, 404.96]$ and a β_D interval of $[-9.6345, 1409.6]$. While the nested sampling results are slowly converging to these intervals, accuracy is limited to only one or two digits after 10^8 samples (highlighted in magenta). The PCE/SC combined expansions using SSG also appear to be slowly converging to the correct reliability index intervals, but upper bound accuracy is poor even at the highest w = 8 level (highlighted in green). In addition, the reliability index upper bounds for most of the SC combined expansions have diverged resulting from negative expansion variance (this cannot happen with PCE, but is possible for SC, particularly for sparse grids when collocation weights can be negative – see Eqs. 27 and 29). Again, the PCE PC regression-based results scale well, but accuracy lags SSG numerical integrations. In addition, the PCE PC combined expansion approach does not appear to be converging, likely due to ill-conditioning in the linear least squares solution. Overall, the SC aleatory expansion approach using SSG is the best performer, with good accuracy at w = 2 at the cost of 2646 evaluations (highlighted in blue).

E. Steel Column

The final analytic test problem involves the trade-off between cost and reliability for a steel column.[39] The cost is defined as

$$Cost = bd + 5h \tag{69}$$

where b, d, and h are the means of the flange breadth, flange thickness, and profile height, respectively. This problem demonstrates the efficiency of different coefficient estimation approaches when scaled to larger dimensional UQ problems. Nine uncorrelated random variables are used in the problem to define the yield stress F_s (lognormal with $\mu/\sigma = 400/35$ MPa), dead weight load P_1 (normal with $\mu/\sigma = 500000/50000$ N), variable load P_2 (gumbel with $\mu/\sigma = 600000/90000$ N), variable load P_3 (gumbel with $\mu/\sigma = 600000/90000$ N), flange breadth B (lognormal with $\mu/\sigma = b/3$ mm), flange thickness D (lognormal with $\mu/\sigma = d/2$ mm), profile height H (lognormal with $\mu/\sigma = h/5$ mm), initial deflection F_0 (normal with $\mu/\sigma = 30/10$ mm), and Youngs modulus E (weibull with $\mu/\sigma = 21000/4200$ MPa). The limit state has the following analytic form:

$$g = F_s - P\left(\frac{1}{2BD} + \frac{F_0}{BDH}\frac{E_b}{E_b - P}\right) \tag{70}$$

where

$$P = P_1 + P_2 + P_3 \tag{71}$$

$$E_b = \frac{\pi^2 EBDH^2}{2L^2} \tag{72}$$

and the column length L is 7500 mm.

As shown in Ref. 5, this problem has a singularity in the limit state out in the (heavy) tails of the input distributions due to subtractive cancellation in the denominator of Eq. 70. Therefore, this function is not in L_2 (does not have finite variance) and UQ convergence studies are not meaningful in the absense of basis sugmentation/discretization techniques to resolve the singularity. However, for a fixed resolution in the stochastic expansions, design under uncertainty studies are still meaningful.

1. *Design under uncertainty*

This design problem demonstrates design variable insertion into random variable distribution parameters through the design of the mean flange breadth, flange thickness, and profile height. Since there are no augmented design variables in this problem, the two design sensitivity approaches collapse into one. The following design formulation maximizes the reliability subject to a cost constraint:

$$\begin{aligned} \max \quad & \beta \\ \text{s.t.} \quad & Cost \leq 4000. \\ & 200.0 \leq b \leq 400.0 \\ & 10.0 \leq d \leq 30.0 \\ & 100.0 \leq h \leq 500.0 \end{aligned} \tag{73}$$

For PCE, the limit state is modeled using a Hermite expansion and the coefficients are estimated using either point collocation with a second-order expansion and oversampling ratio of two or sparse grid level = 2 (which corresponds to a second-order expansion for tailored total-order PCE). For SC, only sparse grid level = 2 is employed. NPSOL SQP is the optimizer, SR1 updates provide quasi-second-order linkages in sequential approaches, and multifidelity approaches employ uncertain expansions as the high fidelity models (mirroring the corresponding bi-level settings) and MVFOSM as the low fidelity models. Table 9 shows the computational results. For this problem, only the SC bi-level uncertain expansion approach (highlighted in

Table 9. PCE-based and SC-based design results, steel column test problem.

OUU Approach	Sensitivity Approach	Expansion Variables	Integration Approach	Evaluations (Fn, Grad)	β	Cost
PCE Bi-level	Analytic	Uncertain	Pt Colloc	(2090, 660)	3.257	4000.
PCE Sequential 1	Analytic	Uncertain	Pt Colloc	(1100, 550)	3.257	4000.
PCE Sequential Q2	Analytic	Uncertain	Pt Colloc	(660, 330)	3.257	4000.
PCE/MV Multifid 1	LF Num, HF Ana	LF MV, HF Unc	Pt Colloc	(863, 533)	3.257	4000.
PCE Bi-level	Analytic	Uncertain	Linear SSG	(2985, 995)	3.237	4000.
PCE Sequential 1	Analytic	Uncertain	Linear SSG	(1990, 995)	3.237	4000.
PCE Sequential Q2	Analytic	Uncertain	Linear SSG	(1194, 597)	3.237	4000.
PCE/MV Multifid 1	LF Num, HF Ana	LF MV, HF Unc	Linear SSG	(1439, 842)	3.237	4000.
SC Bi-level	Analytic	Uncertain	Linear SSG	(2388, 796)	3.036	4000.
SC Sequential 1	Analytic	Uncertain	Linear SSG	(1990, 995)	3.236	4000.
SC Sequential Q2	Analytic	Uncertain	Linear SSG	(1194, 597)	3.236	4000.
SC/MV Multifid 1	LF Num, HF Ana	LF MV, HF Unc	Linear SSG	(1432, 835)	3.236	4000.

red) fails to converge accurately to the optimal design point at $(b, d, h) = (200., 17.5, 100.)$. For all other cases, any discrepancy in the optimal β derives from inaccuracy in the expansion (the fully converged β value for the optimal design point is 3.236). For this higher dimensional problem, regression-based approaches (point collocation) can be seen to scale better than numerical integration approaches (linear SSG), although the accuracy of the SSG approaches is superior. Overall, the PCE/SC quasi-second-order sequential approaches (highlighted in green) are the most efficient approaches, followed by PCE/SC Mean Value-based multifidelity approaches (highlighted in blue).

VII. Conclusions

This paper has investigated the relative performance of non-intrusive generalized polynomial chaos and Lagrange interpolation-based stochastic collocation methods applied to several algebraic benchmark problems with known solutions. The primary distinction between these methods is that PCE must estimate coefficients for a known basis of orthogonal polynomials (using sampling, linear regression, tensor-product quadrature, or Smolyak sparse grids) whereas SC must form an interpolant for known coefficients (using quadrature or sparse grids).

Performance between these methods is shown to be very similar and both demonstrate impressive efficiency relative to Monte Carlo sampling methods and impressive accuracy relative to local reliability methods. When a difference is observed between traditional PCE and SC using the same collocation point sets, SC has been the consistent winner, typically manifesting in the reduction of the required integration by one order or level. This difference can be attributed at least in part to expansion/integration synchronization issues with PCE, motivating approaches for tailoring of chaos expansions that closely synchronize with numerical integration schemes.

For the case of tensor-product quadrature, tailored tensor-product PCE is shown to perform identically to SC such that the performance gap is completely eliminated. Both methods consistently outperform traditional PCE. However, tensor-product quadrature approaches only outperform sparse grid approaches for the lowest dimensional problems.

For problems with greater than two dimensions, Smolyak sparse grid approaches are shown to outperform

tensor-product quadrature approaches. For sparse grids, selection of a synchronized PCE formulation is nontrivial and the tailored total-order PCE approach, which computes the maximal total-order expansion that can be resolved by a particular sparse grid, is shown to be more rigorous and reliable than heuristics and eliminates inefficiency due to trial and error. A significant performance gap relative to SC with sparse grids still remains for the case of nonlinear sparse grid growth rules, but replacement of these rules with linear ones (for Gaussian quadratures that are at most weakly nested) reduces the set of resolvable monomials that do not appear in the total-order expansion, resulting in a further reduction of the performance gap.

While efforts in tailoring the form of the PCE can reduce and in some cases eliminate the performance gap with SC, no nonintrusive PCE approach has been shown to outperform SC when using the same set of collocation points. Rather, usage of PCE remains motivated by other considerations, in particular its greater flexibility in collocation point selection and coefficient estimation approaches. In particular, PCE allows for usage of unstructured/random collocation point sets that can support greater simulation fault tolerance, Genz cubature grids that support more optimal numerical integration than sparse grids, and linear regression approaches that may enable resolution of higher random dimensions and higher expansion orders than sparse grid approaches. In addition, analytic variance-based decomposition and a guarantee of positive expansion variance are also features of PCE not provided by SC. Thus, PCE and SC provide their own sets of strengths and weaknesses and selection between the two approaches remains dependent on the efficiency and flexibility requirements of specific applications.

The preferred UQ approaches (SC with tensor-product quadrature for low dimensions and linear growth Smolyak sparse grids for high dimensions; PCE with tensor-product quadrature for low dimensions and either linear growth Smolyak sparse grids or linear regression for high dimensions) are carried forward in design under uncertainty and epistemic interval estimation studies employing two stochastic sensitivity approaches, one based on expansions of response design sensitivities over aleatory uncertain variables and another based on combined expansions of response functions over aleatory variables and either design or epistemic variables. While it is shown that both approaches are capable of exact results, computational experiments indicate that the former approach is more reliable (so long as the underlying response derivatives are reliable) for use in gradient-based design optimization and nongradient-based interval estimation.

For design under uncertainty, the two stochastic sensitivity approaches provide the foundation for exploration of bi-level, sequential, and multifidelity formulations. Quasi-second order linkages are shown to be preferred to first-order linkages within sequential formulations, and these quasi-second-order sequential approaches are the most efficient on two of the four OUU problems. Multifidelity approaches are shown to be capable of coercing the low fidelity optimization to converge to the high fidelity optimum; however, an inexpensive low fidelity UQ model is shown to be critically important to the overall efficiency of the process. Only the inexpensive Mean Value-based low fidelity UQ resulted in a competitive multifidelity method, and this approach was either most efficient or runner up in three of the four problems. Thus, while neither sequential nor multifidelity OUU approaches consistently outperformed the simpler bi-level approach (when using an efficient gradient-based optimizer such as sequential quadratic programming), both approaches show promise and merit ongoing study and refinement.

For epistemic interval estimation, the goal is to develop second-order probability approaches that can be more accurate (via crisp bounds from optimizers) and more efficient (via exponential convergence rates from stochastic expansion methods) than nested sampling. Initial computational experiments have demonstrated that nongradient-based global optimization combined with the PCE/SC aleatory expansion approach achieves this objective, and provides interval bounds for two model problems using $O(10^2) - O(10^3)$ simulations that are significantly more accurate that those obtainable from $O(10^8)$ simulations in the traditional nested sampling approach. To further reduce expense or to scale to larger problems, one may relax this approach of using global methods at both levels and explore the use of local gradient-based methods within either loop to estimate approximate intervals.

In both OUU and epistemic interval estimation cases, the PCE/SC uncertain/aleatory expansions tend to be more effective than the PCE/SC combined expansions. This is especially true for interval estimation, where the process of globally minimizing and maximizing the statistics of the expansion stresses the models and will tend to seek out any regions where the approximation becomes inaccurate. Whereas the combined expansion results are shown to converge in most cases when provided sufficient refinement, the ability to resolve the aleatory statistics for only selected instances of the nonprobabilistic parameters (aleatory expansions) one at a time appears to be significantly more efficient than attempting to globally resolve these statistics for all values of the nonprobabilistic parameters (combined expansions) all at once.

Acknowledgments

The author thanks Paul Constantine and Gianluca Iaccarino of Stanford University for discussions related to PCE tailoring, Dongbin Xiu of Purdue University for discussions on usage of orthogonal polynomial bases for nonprobabilistic dimensions, John Burkardt of Virginia Tech for development of Gauss point/weight and sparse grid software used for numerical integrations in this work, and Laura Swiler from Sandia for generation of second-order probability results using nested sampling.

References

[1]Xiu, D. and Karniadakis, G. M., "The Wiener-Askey Polynomial Chaos for Stochastic Differential Equations," *SIAM J. Sci. Comput.*, Vol. 24, No. 2, 2002, pp. 619–644.

[2]Askey, R. and Wilson, J., "Some Basic Hypergeometric Polynomials that Generalize Jacobi Polynomials," *Mem. Amer. Math. Soc. 319*, AMS, Providence, RI, 1985.

[3]Wiener, N., "The Homogoeneous Chaos," *Amer. J. Math.*, Vol. 60, 1938, pp. 897–936.

[4]Abramowitz, M. and Stegun, I. A., *Handbook of Mathematical Functions with Formulas, Graphs, and Mathematical Tables*, Dover, New York, 1965.

[5]Eldred, M. S., Webster, C. G., and Constantine, P., "Evaluation of Non-Intrusive Approaches for Wiener-Askey Generalized Polynomial Chaos," *Proceedings of the 10th AIAA Nondeterministic Approaches Conference*, No. AIAA-2008-1892, Schaumburg, IL, April 7–10 2008.

[6]Der Kiureghian, A. and Liu, P. L., "Structural Reliability Under Incomplete Probability Information," *J. Eng. Mech., ASCE*, Vol. 112, No. 1, 1986, pp. 85–104.

[7]Golub, G. H. and Welsch, J. H., "Caclulation of Gauss Quadrature Rules," *Mathematics of Computation*, Vol. 23, No. 106, 1969, pp. 221–230.

[8]Witteveen, J. A. S. and Bijl, H., "Modeling Arbitrary Uncertainties Using Gram-Schmidt Polynomial Chaos," *Proceedings of the 44th AIAA Aerospace Sciences Meeting and Exhibit*, No. AIAA-2006-0896, Reno, NV, January 9–12 2006.

[9]Ghanem, R. G., private communication.

[10]Eldred, M. S., Agarwal, H., Perez, V. M., Wojtkiewicz, Jr., S. F., and Renaud, J. E., "Investigation of Reliability Method Formulations in DAKOTA/UQ," *Structure & Infrastructure Engineering: Maintenance, Management, Life-Cycle Design & Performance*, Vol. 3, No. 3, 2007, pp. 199–213.

[11]Eldred, M. S. and Bichon, B. J., "Second-Order Reliability Formulations in DAKOTA/UQ," *Proceedings of the 47th AIAA/ASME/ASCE/AHS/ASC Structures, Structural Dynamics and Materials Conference*, No. AIAA-2006-1828, Newport, RI, May 1–4 2006.

[12]Rosenblatt, M., "Remarks on a Multivariate Transformation," *Ann. Math. Stat.*, Vol. 23, No. 3, 1952, pp. 470–472.

[13]Box, G. E. P. and Cox, D. R., "An Analysis of Transformations," *J. Royal Stat. Soc.*, Vol. 26, 1964, pp. 211–252.

[14]Rackwitz, R. and Fiessler, B., "Structural Reliability under Combined Random Load Sequences," *Comput. Struct.*, Vol. 9, 1978, pp. 489–494.

[15]Chen, X. and Lind, N. C., "Fast Probability Integration by Three-Parameter Normal Tail Approximation," *Struct. Saf.*, Vol. 1, 1983, pp. 269–276.

[16]Wu, Y.-T. and Wirsching, P. H., "A New Algorithm for Structural Reliability Estimation," *J. Eng. Mech., ASCE*, Vol. 113, 1987, pp. 1319–1336.

[17]Nobile, F., Tempone, R., and Webster, C. G., "A Sparse Grid Stochastic Collocation Method for Partial Differential Equations with Random Input Data," *SIAM J. on Num. Anal.*, 2008, To appear.

[18]Nobile, F., Tempone, R., and Webster, C. G., "An Anisotropic Sparse Grid Stochastic Collocation Method for Partial Differential Equations with Random Input Data," *SIAM J. on Num. Anal.*, 2008, To appear.

[19]Gerstner, T. and Griebel, M., "Numerical integration using sparse grids," *Numer. Algorithms*, Vol. 18, No. 3-4, 1998, pp. 209–232.

[20]Smolyak, S., "Quadrature and interpolation formulas for tensor products of certain classes of functions," *Dokl. Akad. Nauk SSSR*, Vol. 4, 1963, pp. 240–243.

[21]Barthelmann, V., Novak, E., and Ritter, K., "High dimensional polynomial interpolation on sparse grids," *Adv. Comput. Math.*, Vol. 12, No. 4, 2000, pp. 273–288, Multivariate polynomial interpolation.

[22]Frauenfelder, P., Schwab, C., and Todor, R. A., "Finite elements for elliptic problems with stochastic coefficients," *Comput. Methods Appl. Mech. Engrg.*, Vol. 194, No. 2-5, 2005, pp. 205–228.

[23]Xiu, D. and Hesthaven, J., "High-order collocation methods for differential equations with random inputs," *SIAM J. Sci. Comput.*, Vol. 27, No. 3, 2005, pp. 1118–1139 (electronic).

[24]Wasilkowski, G. W. and Woźniakowski, H., "Explicit Cost Bounds of Algorithms for Multivariate Tensor Product Problems," *Journal of Complexity*, Vol. 11, 1995, pp. 1–56.

[25]Walters, R. W., "Towards Stochastic Fluid Mechanics via Polynomial Chaos," *Proceedings of the 41st AIAA Aerospace Sciences Meeting and Exhibit*, No. AIAA-2003-0413, Reno, NV, January 6–9, 2003.

[26]Hosder, S., Walters, R. W., and Balch, M., "Efficient Sampling for Non-Intrusive Polynomial Chaos Applications with Multiple Uncertain Input Variables," *Proceedings of the 48th AIAA/ASME/ASCE/AHS/ASC Structures, Structural Dynamics, and Materials Conference*, No. AIAA-2007-1939, Honolulu, HI, April 23–26, 2007.

[27]Sudret, B., "Global sensitivity analysis using polynomial chaos expansions," *Reliability Engineering and System Safety*, Vol. 93, 2008.

[28]Reagan, M. T., Najm, H. N., Pebay, P. P., Knio, O. M., and Ghanem, R. G., "Quantifying Uncertainty in Chemical Systems Modeling," *Int. J. Chem. Kinet.*, Vol. 37, 2005, pp. 368–382.

[29]Wu, Y.-T., Shin, Y., Sues, R., and Cesare, M., "Safety-Factor Based Approach for Probability-Based Design Optimization," *Proceedings of the 42rd AIAA/ASME/ASCE/AHS/ASC Structures, Structural Dynamics, and Materials Conference*, No. AIAA-2001-1522, Seattle, WA, April 16–19, 2001.

[30]Du, X. and Chen, W., "Sequential Optimization and Reliability Assessment Method for Efficient Probabilistic Design," *J. Mech. Design*, Vol. 126, 2004, pp. 225–233.

[31]Eldred, M. S. and Dunlavy, D. M., "Formulations for Surrogate-Based Optimization with Data Fit, Multifidelity, and Reduced-Order Models," *Proceedings of the 11th AIAA/ISSMO Multidisciplinary Analysis and Optimization Conference*, No. AIAA-2006-7117, Portsmouth, VA, September 6–8 2006.

[32]Eldred, M. S., Giunta, A. A., and Collis, S. S., "Second-Order Corrections for Surrogate-Based Optimization with Model Hierarchies," *Proceedings of the 10th AIAA/ISSMO Multidisciplinary Analysis and Optimization Conference*, Albany, NY,, Aug. 30–Sept. 1, 2004, AIAA Paper 2004-4457.

[33]Swiler, L. P., Paez, T. L., and Mayes, R. L., "Epistemic Uncertainty Quantification Tutorial," *Proceedings of the IMAC XXVII Conference and Exposition on Structural Dynamics*, No. paper 294, Orlando, FL, February 2009.

[34]Eldred, M. S., Adams, B. M., Haskell, K., Bohnhoff, W. J., Eddy, J. P., Gay, D. M., Hart, W. E., Hough, P. D., Kolda, T. G., Swiler, L. P., and Watson, J.-P., "DAKOTA, A Multilevel Parallel Object-Oriented Framework for Design Optimization, Parameter Estimation, Uncertainty Quantification, and Sensitivity Analysis: Version 4.2 Users Manual," Tech. Rep. SAND2006-6337, Sandia National Laboratories, Albuquerque, NM, 2008.

[35]Eldred, M. S. and Burkardt, J., "Comparison of Non-Intrusive Polynomial Chaos and Stochastic Collocation Methods for Uncertainty Quantification," *to appear in Proceedings of the 47th AIAA Aerospace Sciences Meeting and Exhibit*, No. AIAA-2009-0976, Orlando, FL, January 5–8, 2009.

[36]Eldred, M. S., Webster, C. G., and Constantine, P., "Design Under Uncertainty Employing Stochastic Expansion Methods," *Proceedings of the 12th AIAA/ISSMO Multidisciplinary Analysis and Optimization Conference*, No. AIAA-2008-6001, Victoria, British Columbia, September 10–12, 2008.

[37]Constantine, P. and Iaccarino, G., "Comparing spectral Galerkin and spectral collocation methods for parameterized matrix equations." Tech. Rep. UQ-08-02, Stanford University, Stanford, CA, 2008.

[38]Schittkowski, K., *More Test Examples for Nonlinear Programming, Lecture Notes in Economics and Mathematical Systems, Vol. 282*, Springer-Verlag, Berlin, 1987.

[39]Kuschel, N. and Rackwitz, R., "Two Basic Problems in Reliability-Based Structural Optimization," *Math. Method Oper. Res.*, Vol. 46, 1997, pp. 309–333.

[40]Sues, R., Aminpour, M., and Shin, Y., "Reliability-Based Multidisciplinary Optimization for Aerospace Systems," *Proceedings of the 42rd AIAA/ASME/ASCE/AHS/ASC Structures, Structural Dynamics, and Materials Conference*, No. AIAA-2001-1521, Seattle, WA, April 16–19, 2001.